Marine Micropaleontology
January 2018, Volume 138 Pages 46-62
https://doi.org/10.1016/j.marmicro.2017.10.003
https://archimer.ifremer.fr/doc/00457/56889/

Ultrastructure and distribution of kleptoplasts in benthic foraminifera from shallow-water (photic) habitats

Jauffrais Thierry [1, *], Lekieffre Charlotte [2], Koho Karoliina A. [3], Tsuchiya Masashi [4], Schweizer Magali [1], Bernhard Joan M. [5], Meibom Anders [2, 6], Geslin Emmanuelle [1]

[1] Univ Angers, UMR CNRS LPG BIAF 6112, Bioindicateurs Actuels & Fossiles, 2 Blvd Lavoisier, F-49045 Angers 1, France.
[2] Ecole Polytech Fed Lausanne, Sch Architecture Civil & Environm Engn ENAC, Lab Biol Geochem, CH-1015 Lausanne, Switzerland.
[3] Univ Helsinki, Dept Environm Sci, Viikinkaari 1, Helsinki, Finland.
[4] Japan Agcy Marine Earth Sci & Technol, Dept Marine Biodivers Res, 2-15 Natsushima Cho, Yokosuka, Kanagawa, Japan.
[5] Woods Hole Oceanog Inst, Dept Geol & Geophys, Woods Hole, MA 02543 USA.
[6] Univ Lausanne, Inst Earth Sci, Ctr Adv Surface Anal, Lausanne, Switzerland.

* Corresponding author : Thierry Jauffrais, email address : Thierry.jauffrais@univ-angers.fr

Abstract :

cAssimilation, sequestration and maintenance of foreign chlbroplasts made an organism is termed "chloroplast sequestration" or "kleptoplasty". This phenomenon is known in certain benthic foraminifera, in which such kleptoplasts can be found both intact and functional, but with different retention times depending on foraminiferal species. In the present study, seven species of benthic foraminifera (Haynesina germanica, Elphidium williamsoni, E. selseyense, E. oceanense, E. aff. E. dispirit, Planoglabratella opercularis and Ammonia sp.) were collected from shallow-water benthic habitats and examined with the transmission electron microscope (TEM) for cellular ultrastructure to ascertain attributes of kleptoplasts. Results indicate that all these foraminiferal taxa actively obtain kleptoplasts but organized them differently within their endoplasm. In some species, the kleptoplasts were evenly distributed throughout the endoplasm (e.g., H. germanica, E. oceanense, Ammonia sp.), whereas other species consistently had plastids distributed close to the external cell membrane (e.g., Elphidium williamsoni, E. selseyense, P. opercularis). Chloroplast degradation also seemed to differ between species, as many degraded plastids were found in Ammonia sp. and E. oceanense compared to other investigated species. Digestion ability, along with different feeding and sequestration strategies may explain the differences in retention time between taxa. Additionally, the organization of the sequestered plastids within the endoplasm may also suggest behavioral strategies to expose and/or protect the sequestered plastids to/from light and/or to favor gas and/or nutrient exchange with their surrounding habitats.

Highlights

► Seven species of benthic foraminifera were examined with the TEM ► The distribution of sequestered chloroplasts was species specific ► Some were evenly distributed throughout the endoplasm ► Others were distributed close to the external cell membrane ► Organization of the kleptoplasts suggests behavioral strategies

Keywords : Kleptoplasty, Probst, Chloroplast, TEM, Transmission electron microscope

1. Introduction

Some benthic foraminiferal species have the ability to steal and sequester chloroplasts (which then become "kleptoplasts") from their microalgal food sources. These foraminiferal species mainly ingest diatoms (Knight and Mantoura, 1985; Bernhard and Bowser 1999, Goldstein et al., 2004; Pillet et al., 2011; Tsuchiya et al., 2015; Jauffrais et al., 2017) but have different strategies for feeding and sequestration (Lopez, 1979; Grzymski et al., 2002; Austin et al., 2005; Jauffrais et al., 2016b). In some foraminiferal species, the kleptoplasts are degraded within hours, possibly as a result of a digestive process, while in other species they are kept and/or remain functional for weeks to months (Lopez, 1979; Lee et al., 1988; Cedhagen, 1991; Correia and Lee, 2000, 2002a, b; Grzymski et al., 2002; Tsuchiya et al., 2015; Jauffrais et al., 2016b). A kleptoplast is thus a chloroplast, functional or not, that was "stolen", integrated and sometimes used by a host organism (Clark et al., 1990). Benthic foraminiferal kleptoplasty is observed in species from different environments: shallow to deep-sea, oxic to anoxic and photic to aphotic habitats (Lopez, 1979; Alexander and Banner, 1984; Lee et al., 1988; Bernhard and Alve, 1996; Bernhard and Bowser, 1999; Bernhard et al., 2000; Correia and Lee, 2000). The photosynthetic function of kleptoplasts has been demonstrated in some shallow-water benthic foraminifera (e.g., *Elphidium williamsoni* and *Haynesina germanica* in Cesbron et al., 2017; Jauffrais et al., 2016; Lopez, 1979). Nevertheless, it remains unknown why certain deep-sea foraminifera sequester chloroplasts as light is absent in their habitat (Bernhard and Bowser, 1999; Grzymski et al., 2002).

In photic shallow-water habitats (e.g., estuaries, bays, lagoons and other intertidal or shallow-water subtidal areas), kleptoplastic benthic foraminiferal species, such as *Haynesina germanica, Elphidium williamsoni,* the "*excavatum*" species complex (e.g., *E. oceanense*, *E. selseyense*, see Darling et al. (2016)), or *Ammonia* spp., are often the dominant mudflat foraminiferal taxa (Debenay et al., 2000; Debenay et al., 2006; Morvan et al., 2006; Bouchet et al., 2009; Pascal et al., 2009; Thibault de Chanvalon et al., 2015; Cesbron et al., 2016). Their vertical distribution is characterized by a clear maximum density in the upper oxygenated millimeters of the sediment (Alve and Murray, 2001; Bouchet et al., 2009; Thibault de Chanvalon et al., 2015; Cesbron et al., 2016), where light can also penetrate (Kuhl et al., 1994; Cartaxana et al., 2011). However, in some kleptoplastic species (e.g., the

morphospecies *A. tepida* and *E. excavatum*) kleptoplasts lack photosynthetic activity (Lopez, 1979; Jauffrais et al., 2016), and in many other kleptoplastic species, the photosynthetic activity has not yet been assessed and/or quantified.

The observed differences in the maintenance of the kleptoplasts suggest there must be substantial differences between kleptoplastic shallow-water foraminiferal species. It is, therefore, necessary to understand the sequestration mechanism in kleptoplastic foraminifera that have similar food sources and environments, but may have different chloroplast-retention times. In this study, we used transmission electron microscope (TEM) to document the ultrastructure and cellular organization of different kleptoplastic foraminifera from shallow-water photic habitats to assess chloroplast organization and degradation processes. In parallel, individuals from the same populations as the ultrastructurally examined specimens have been genetically characterized with DNA barcoding to ascertain their taxonomic identity to ease future comparisons.

2. Material and methods

2.1. Specimen collection and field sample fixations

We examined seven species of living shallow-water benthic foraminifera: *Haynesina germanica* (Fig. 1 and 2), *Elphidium williamsoni* (Fig. 3), *Elphidium oceanense* (Fig. 4), *Elphidium selseyense* (Fig. 5), *Elphidium* aff. *E. crispum* (Fig. 6), *Planoglabratella opercularis* (Fig. 7 and 8) and *Ammonia* sp. phylotype T6 (Fig. 9 and 10).

Haynesina germanica (4 specimens ultrathin sectioned and observed by TEM), *E. oceanense* (3 specimens ultrathin sectioned and observed by TEM) and *Ammonia* sp. (3 specimens ultrathin sectioned and observed by TEM) were collected from the Bourgneuf Bay tidal mudflat (Bay of Biscay, south of the Loire estuary, France), a 11 AM from surface sediments (~0-0.5 cm depth, temperature of the sediment 11°C, salinity 31) in March 2016 at low tide during a cloudy day. The foraminifera-bearing sediments were fixed in the field immediately after sampling, with a fixative solution containing 4% glutaraldehyde and 2% paraformaldehyde in artificial seawater (Red Sea® salt in MilliQ® water at salinity 35). The samples were then kept at room temperature (18-20°C) for 24 h and subsequently placed at 4°C until further processing.

104 *Haynesina germanica* (3 specimens ultrathin sectioned and observed by TEM) and *E. selseyense* (1
105 specimen ultrathin sectioned and observed by TEM) were isolated in February 2016 from two Wadden
106 Sea tidal mudflats during low tide (Texel Island, the Netherlands): Mokbaai (sediment temperature =
107 4°C, salinity = 27, at 7:30AM on a sunny day) and Cocksdorp (sediment temperature = 4°C, salinity =
108 23, at 8AM on a sunny day). Sediment cores were sliced at 1-cm intervals down to 10-cm depth. The
109 top 1-cm of each sediment core was sieved over a 125-µm screen and foraminifera containing healthy
110 looking cytoplasm were picked within 30 h of sampling from the >125-µm fraction under illuminated
111 binocular microscope. The vitality of all isolated foraminifera was further assessed based on
112 movements as outlined in Koho et al. (2011). Immediately after vitality checks, living specimens were
113 transferred to a fixative solution containing 2% glutaraldehyde and 4% paraformaldehyde in filtered
114 seawater and stored at 4°C. After 24 h, the specimens were transferred into a solution containing 4%
115 paraformaldehyde in filtered seawater and stored at 4°C, where they remained until further processing.
116 *Elphidium williamsoni* (5 specimens ultrathin sectioned and observed by TEM) were collected from
117 surface sediments (0-0.5 cm depth) in May 2016 from a small tidal mudflat at low tide 2 PM, on a
118 sunny day in Fiskebäckskil near Kristineberg Marine Research Station (Gullmar Fjord, Sweden). The
119 sediments with foraminifera were fixed and preserved immediately in the field as noted for *H.*
120 *germanica* from the Bourgneuf Bay tidal mudflat.
121 *Elphidium* aff. *E. crispum* (12 specimens ultrathin sectioned and observed by TEM) and *P. opercularis*
122 (12 specimens ultrathin sectioned and observed by TEM) were isolated from coralline algae
123 (*Corallina pilulifera*, Rhodophyta) collected from rocky shores of Yugawara (Kanagawa Prefecture,
124 Japan) in May 2012 at 1 m depth. The vitality of all isolated foraminifera was assessed based on
125 pseudopodial extension using an inverted microscope with a phase-contrast apparatus. Living
126 specimens were picked with a fine (soft) needle, fixed for 2 h in 2.5% seawater-buffered
127 glutaraldehyde and then transferred in filtered (0.2 µm) seawater and kept at 4°C until processing.
128
129 *2.2. Species identifications*

Specimens were taxonomically identified based solely on the morphology of the test as revealed with a scanning electron microscope (SEM) or based on both morphology (SEM micrographs) and molecular (DNA barcoding; DNA sequences) tools.

For the Bay of Bourgneuf and the Gullmar Fjord, foraminifera from the same sampling of specimens used for the TEM studies were selected for DNA barcoding (Table 1). Live foraminifera were picked from the sediment, dried on micropaleontological slides, imaged with an environmental SEM (EVO LS10, ZEISS) and individually extracted for DNA in Deoxycholate (DOC) buffer (e.g., Pawlowski, 2000; Schweizer et al., 2011). For the DNA amplification, a fragment situated at the 3' end of the small subunit (SSU) rDNA was selected because this region is the barcode for foraminifera (Pawlowski and Holzmann, 2014). The primer pairs were s14F3 and J2 for the primary polymerase chain reactions (PCR) and s14F1 and N6 for the secondary (nested) PCR (Pawlowski, 2000; Darling et al., 2016). Positive PCR gave a fragment of about 500 nucleotides (nt) that was purified and sequenced directly as described in Schweizer et al. (2011).

New DNA sequences were deposited in GenBank (accession numbers KY347797-KY347800).

For the Dutch and Japanese specimens, available DNA sequences (Schweizer et al., 2008; Schweizer et al., 2011; Tsuchiya et al., 2000; Pawlowski and Holzmann, unpublished data) were gathered from GenBank (Table 1).

The sequences retrieved from the studied species (Table 1) were then compared to published sequences (Hayward et al., 2004; Darling et al., 2016) within an alignment obtained with SeaView (Gouy et al., 2010) to identify them molecularly.

2.3. Ultrastructural observations by TEM

Chemically preserved specimens were rinsed in filtered seawater and then either decalcified in 0.1 or 0.5 M ethylenediamine tetraacetic acid (EDTA) prepared in distilled water (pH 7.4) and post-fixed with 2% osmium tetroxide (OsO_4) solution prepared in filtered seawater for about 1-2 h, or the reverse (both processes worked). Foraminifera were then dehydrated with successive ethanol baths and embedded in resin, either Epon (Epon 812 resin, TAAB) or LR White® (Sigma-Aldrich). Ultra-thin sections (60-70 nm) were prepared with an ultra-microtome (Reichert Ultracut S, Leica) after staining

158 with uranyl acetate, or with 1% aqueous uranyl acetate and 0.5% lead citrate, and then coated with
159 carbon using a JEE-400 high vacuum evaporator (JEOL Ltd). The ultrathin sections were finally
160 examined with either a JEM-1400 (JEOL Ltd), JEM-1210 (JEOL Ltd) or TECNAI G2 20 (FEI
161 Company) TEM at an acceleration voltage of 80-100kV.
162
163 **3. Results and discussion**
164 This contribution presents the ultrastructure and cellular distribution of kleptoplasts, highlighting
165 differences in chloroplast organization and degradation processes in foraminifera from shallow-water
166 habitats (synopsis in Table 2). The description and organization of other organelles in benthic
167 foraminifera are described in detail elsewhere (see, LeKieffre et al., this issue).
168
169 *3.1. Haynesina germanica* (Fig. 1 and 2)
170 *Haynesina germanica* is relatively easy to recognize morphologically and there is good congruence
171 between morphological and molecular identification (Darling et al., 2016, phylotype S16);
172 consistently, we found good agreement between the molecular and morphological identification of the
173 specimens collected from the Bourgneuf Bay tidal mudflat (France). Direct molecular identification
174 was not performed on specimens collected from Texel (Mokbaai, NL). However, specimens from a
175 nearby site (Wadden Sea, Den Oever, NL) that were sequenced and identified as phylotype S16
176 (Schweizer et al., 2011, Table 1) bore similar morphology to Mokbaai specimens.
177 In all four specimens studied with TEM, the kleptoplasts were evenly distributed in each chamber and
178 large vacuoles were also densely and evenly distributed (Fig. 1B, C and Fig. 2B). The chloroplasts
179 showed fine structural details and were relatively well preserved in the foraminiferal endoplasm with
180 thylakoids, girdle lamella surrounding each kleptoplast and pyrenoids (Fig. 1E, F, and Fig. 2C, E). The
181 pyrenoids were also well preserved, often transected by a lamella and surrounded by another lamella
182 (Fig. 1E, F and Fig. 2C, E). Ideally in *H. germanica*, five membranes are visible around the
183 chloroplast; the four inner membranes are most likely those of the diatom and the fifth and outermost
184 membrane is that of the foraminifer (Goldstein et al., 2004). In the present study, an electron-lucent
185 space was often observed between the chloroplast membranes and the host membrane (Fig. 1 D, E and

F, and Fig. 2E). This electron-lucent space may be an artefact caused by the chemical fixation and embedding procedures.

3.2. Elphidium williamsoni (Fig. 3)

The morphospecies *Elphidium williamsoni* has been formally linked to phylotype S1 (Darling et al., 2016) with DNA sequencing of topotypic specimens (Roberts et al., 2016). A specimen from the Gullmar Fjord sample was also sequenced and found to belong to phylotype S1 (Table 1), confirming the morphological determination.

Kleptoplasts were abundant and situated just below the cell periphery (Fig. 3B, C) or close to it (Fig. 3D). Kleptoplasts were also well preserved with pyrenoid, lamella and thylakoids (Fig. 3E, F). A degraded kleptoplast at the foraminiferal cell periphery had inter-thylakoid spaces (Fig. 3C (c*)). As observed in *H. germanica,* the kleptoplasts were surrounded by host membrane, with electron-lucent spaces between the chloroplasts and the endoplasm of the host (Fig. 3B to F) that may be an artefact caused by the chemical fixation and embedding procedures.

3.3. Elphidium "excavatum" species complex (Fig. 4 and 5)

Elphidium oceanense and *E. selseyense* belong to the "*excavatum*" species complex as defined by Darling et al. (2016). The morphospecies *Elphidium excavatum* was thought to include a large number of ecophenotypes due to its high morphological diversity. However, recent molecular phylogenetics studies have shown that this morphospecies is actually a species complex (Schweizer et al., 2011; Pillet et al., 2013; Darling et al., 2016). These species are pseudocryptic, meaning that a careful morphological examination of specimens traditionally determined as *E. excavatum* allows classification to one species of the complex (Darling et al., 2016). Presently, four different phylotypes have been identified and linked to previously described morphological forms that were then given species status: S3=*E. oceanense*, S4=*E. clavatum*, S5=*E. selseyense*, S13=*E. lidoense* (Darling et al., 2016).

3.3.1. *Elphidium oceanense* (Fig. 4)

214 Specimens collected from the Bourgneuf Bay tidal mudflat, France, were morphologically and
215 molecularly identified as phylotype S3 in Darling et al. (2016). This phylotype is the most common
216 member of the "*excavatum*" species complex in the Bourgneuf Bay tidal mudflat (Schweizer et al.,
217 unpublished results and Table 1).
218 In *E. oceanense,* kleptoplasts and vacuoles were evenly and densely distributed in the endoplasm (Fig.
219 4C, D). The kleptoplasts were in large vacuoles containing numerous plastids and fine materials (Fig.
220 4D - F). The plastids often appeared in a degraded state with small circular electron-lucent disruptions
221 of thylakoids and pyrenoids (Fig. 4E, F). Kleptoplast pyrenoids, lamella and thylakoids remained
222 clearly distinguishable (Fig. 4E, F).
223
224 3.3.2. *Elphidium selseyense* (Fig. 5)
225 The specimens from Cocksdorp (Wadden Sea) were identified morphologically as *E. selseyense.* This
226 species, which is linked to the phylotype S5 (Darling et al., 2016), was isolated in 1999 from the same
227 location (Schweizer et al., 2011; Table 1). *Elphidium selseyense* is known as a widespread and
228 opportunistic species with ecology similar to the other species described above (Murray, 1991; Horton
229 and Edwards, 2006; Darling et al., 2016).
230 Specimens of *E. selseyense* had many kleptoplasts situated immediately below the host-cell periphery
231 (Fig. 5B, C and D) with relatively fewer chloroplasts internally in the endoplasm (Fig. 5B).
232 Kleptoplasts exhibited a girdle lamella, a simple pyrenoid, thylakoids and also osmiophilic globules
233 (Bedoshvili et al., 2009), which could be lipoprotein particles such as plastoglobules as suggested
234 previously by Leutenegger (1977) and Schmaljohann and Röttger (1978).
235 Despite being phylogenetically closely related (Darling et al. 2016), *E. oceanense* and *E. selseyense*
236 clearly have different chloroplast sequestration strategies. First, the plastids were distributed
237 throughout cytoplasm in *E. oceanense* compared to *E. selseyense,* where the plastids occurred
238 peripherally. Second, the kleptoplasts were relatively degraded in *E. oceanense* and relatively intact in
239 *E. selseyense*. Third, multiple plastids occurred in one vacuole of *E. oceanense* whereas, typically, a
240 single plastid was seen in one vacuole of *E. selseyense*. These differences suggest that, in *E.*
241 *oceanense,* the kleptoplasts were not functional, whereas, in *E. selseyense* they may still be functional,

242 possibly producing oxygen and assimilating inorganic carbon and nitrogen. Although these two
243 *Elphidium* taxa are within the same species complex as defined by Darling et al. (2016), differences in
244 chloroplast maintenance and distribution reveal that the species differ not only genetically and
245 morphologically, but also physiologically. Such observations emphasize the need to clearly identify
246 individuals within this species complex. These differences within the same species complex also
247 hamper direct comparison with previous studies on *E. excavatum* structures (Lopez, 1979; Correia and
248 Lee, 2000, 2002a, b) where no morphological (SEM images) and/or molecular (sequence) data are
249 available.
250
251 *3.4. Elphidium* aff. *E. crispum* (Fig. 6)
252 Specimens of *E.* aff. *E. crispum* were isolated from intertidal rocky shores of Yugawara (Kanagawa
253 Prefecture, Japan) where they are commonly encountered living on coralline algae (Kitazato, 1994).
254 No published sequence data is yet available for this species, but the preliminary analysis of the
255 sequences differs from the European *E. crispum* (phylotype S11, Darling et al., 2016 and Tsuchiya,
256 unpubl. data), therefore explaining the use of open nomenclature here.
257 Kleptoplasts were evenly and densely distributed in the endoplasm (Fig. 6B, C, F). Some organelles
258 such as mitochondria, Golgi apparatus, and peroxisomes were found near the kleptoplasts (Fig. 6D).
259 The kleptoplasts appear singly in vacuoles and have a girdle lamella, thylakoids, and pyrenoid divided
260 in two by a lamella and the presence of osmiophilic globules (Fig. 6E and G). Kleptoplasts were noted
261 in different states of degradation (Fig. 6H).
262
263 *3.5. Planoglabratella opercularis* (Fig. 7 and 8)
264 *Planoglabratella opercularis* is also commonly encountered in the intertidal zone of rocky shores
265 around the Japanese Islands where it lives on thalli of coralline algae (Kitazato, 1988; Tsuchiya et al.,
266 2014). Specimens collected near the TEM-sample collection site have been sequenced previously for
267 the large subunit (LSU) and SSU rDNA (Tsuchiya et al., 2000 see Table 1) and Internal transcribed
268 spacer (ITS) rDNA sequences (Tsuchiya et al., 2003; Tsuchiya et al., 2014, see Table 1). Moreover,
269 SSU rDNA sequences of *P. opercularis* from China have now been deposited in GenBank

(LN714815-LN714825; Holzmann and Pawlowski, 2017). The LSU rDNA sequence of a deposited Chinese specimen is identical to LSU sequences of the Japanese *P. opercularis* (Table 1).

Because *P. opercularis* is trochospiral with an attached mobile mode of life and directly exposed to sunlight, chloroplast distribution and sequestration are discussed in the context of spiral, umbilical and lateral perspectives, respectively (Fig. 7A-C). Kleptoplasts were situated at the proximity of the foraminifer's spiral surface, close to the pores and pores plates, where they formed a continuous layer of chloroplasts (Fig. 7B and Fig.8A, B). Also, some of the plastids were distributed in the endoplasm but at a lower density (Fig. 7B, 8E). Surrounding organelles such as mitochondria and Golgi apparatus were also found close to the kleptoplasts (Fig. 7F). The kleptoplasts were well preserved with thylakoids and a pyrenoid (Fig. 7C, D, F). Such peripheral distributions suggest active strategies of *P. opercularis* to maximise light acquisition by the kleptoplast, to favor gas (e.g., O_2, CO_2) and/or dissolved nutrient (e.g., nitrogen) exchanges with their surrounding habitats.

3.6. Ammonia sp. (phylotype T6, Fig. 9 and 10)

Ammonia isolated in Bourgneuf Bay tidal mudflat (France) were first identified as the morphospecies *A. tepida* (Jauffrais et al., 2016a). This morphospecies, however, is polyphyletic, with morphologically identical specimens belonging to distantly related species genetically (Hayward et al., 2004). Specimens from the same sample as the TEM-studied ones were sequenced (Schweizer et al., unpublished results and Table 1) and identified as *Ammonia* sp. (phylotype T6, Hayward et al., 2004).

Kleptoplasts were evenly distributed through chambers, along with diatom frustules and large vacuoles (Fig. 9B). An entire section of a diatom was noted in the endoplasm of one host (Fig. 9D). In this case, the degradation of the diatom had begun because the diatom cell had shrunken within the frustule, however, the detailed intracellular organization of the diatom remained clearly visible. Two chloroplasts with a simple pyrenoid were observable; they were linked by a bridge of cytoplasm where a nucleus and small vacuoles were also visible. A thin layer of cytoplasm then extended to the ends of the cell surrounding two large vacuoles and mitochondria.

Kleptoplasts of *Ammonia* sp. appeared in different states of degradation (Fig. 10). In well-preserved kleptoplasts, the pyrenoid was separated by a lamella composed of a thylakoid and surrounded by an

298 electron-lucent lamella (Fig. 10A). The thylakoids and girdle lamella were also visible (Fig. 10A and
299 B). In degraded kleptoplasts, the structure of the thylakoids and pyrenoid was disrupted and the
300 lamellae were degraded. These degraded kleptoplasts had inter-thylakoid spaces (Fig. 10C and D).
301 Their degradation state and the fact that *Ammonia* sp. kleptoplasts are known to quickly become non-
302 functional (Jauffrais et al., 2016b) suggest that this species merely feeds on diatoms and does not
303 sequester chloroplasts to perform photosynthesis.
304
305 *3.7. General discussion*
306 Our findings indicate that all seven foraminiferal taxa studied actively sequester chloroplasts but
307 sequestration strategies differed between species.
308 Firstly, the structure of the pyrenoid (one transecting lamella surrounded by one membrane), the
309 presence of a girdle lamella and, thylakoids, and the absence of starch accumulation, together other
310 evidence (ultrastructural, pigment and molecular analyses of the sequestered plastids, Goldstein et al.,
311 2004; Knight and Mantoura, 1985; Pillet et al., 2011, Jauffrais et al. 2016), suggest that the
312 kleptoplasts in all seven species belonged to diatoms. Similar ultrastructural, pigment and molecular
313 analyses confirm a similar source for deep-water kleptoplastic benthic foraminifera (Bernhard and
314 Bowser 1999; Grzymski et al., 2001). Secondly, kleptoplast distributions within the endoplasm
315 differed. In some species, the kleptoplasts were evenly distributed (e.g., *H. germanica*, *E. oceanense*
316 and *Ammonia* sp.), whereas in other species the plastids were located close to the cell periphery (e.g.,
317 *E. williamsoni*, *E. selseyense*, *P. opercularis*) and pore-plate complexes (e.g., *P. opercularis*). The
318 differences in the organization of plastids within the endoplasm suggest different behavioral strategies,
319 which expose and/or protect the sequestered plastids to/from light, and can favor gas (e.g., O_2, CO_2)
320 and dissolved nutrient (e.g., ammonium, nitrate) exchange with their surrounding habitats. Peripheral
321 chloroplast distributions might be considered as an active strategy of the foraminifer (e.g., *E.*
322 *williamsoni*, *E. selseyense*, *P. opercularis*) to maximize light acquisition by kleptoplasts. In contrast,
323 an internal distribution of kleptoplasts (e.g., *H. germanica*, *E. oceanense* and *Ammonia* sp.) could be
324 considered either as an absence of strategy, as a strategy to protect the kleptoplasts from an excess of
325 light and/or as an alternative strategy to maximize light exposure by continuously moving kleptoplasts

in the endoplasm of the cell to modulate light exposure. These results emphasize that studies on kleptoplast ultrastructure of benthic foraminifera must be interpreted with care, as results on their distribution might be influenced by the foraminiferal light exposure in the field and/or during experimental studies. Contrary to the present study were the ambient light intensity before fixation is unknown. We thus recommend for future ultrastructural studies to include control, or measure of light intensity. In any case, the clear difference in the chloroplast organization between two phylogenetically closely related species, *E. oceanense* and *E. selseyense* (Darling et al., 2016), lends a novel (physiological) attribute distinguishing the two species beyond genetics and morphology.

Thirdly, chloroplast degradation timescale and the processes involved seem to be species specific as many degraded plastids were found in *E. oceanense* and *Ammonia* sp. compared to other species. Furthermore, the presence of numerous degraded chloroplasts in the endoplasm of *Ammonia* sp. and *E. oceanense* is consistent with the absence of photosynthetic activity in both of these species (Lopez, 1979; Jauffrais et al., 2016b).

Finally, ingestion and sequestration strategies also differed among taxa. Diatom frustules were only found in *Ammonia* sp. while other species had isolated plastids lacking frustules. Another distinguishing characteristic could be the number of sequestered plastids (single to multiple) surrounded by a single host membrane. Such variations may be related to differences in chloroplast maintenance between foraminiferal species.

Acknowledgements

The authors thank Romain Mallet, Florence Manero, and Guillaume Mabilleau for their help at the Imaging core facility (SCIAM laboratory) of the University of Angers, and Sophie Quinchard (UMR 6112 LPG-BIAF) for her technical help in the molecular identification of the different foraminiferal species. TJ was funded by the "FRESCO" project, a project supported by the Region Pays de Loire and the University of Angers. This work was also supported by a grant no. 200021_149333 from the Swiss National Science Foundation and the French national program EC2CO-LEFE (project ForChlo).JMB acknowledges the Robert W. Morse Chair for Excellence in Oceanography and the Investment in Science Fund at WHOI. Also, KK acknowledges the Academy of Finland (Project

354 numbers: 278827, 283453), the electron Microscopy unit of University of Helsinki and the
355 Netherlands Institute for Sea Research for funding, preparation and assistance with TEM and SEM
356 images, and for providing facilities to conduct fieldwork in the Dutch Wadden Sea. MT thanks
357 Katsuyuki Uematsu and Akihiro Tame (Marine Works Japan, Ltd) for their help with TEM
358 preparations. The authors would like to thank Prof Richard Jordan for editing this article.
359

360 **References**

361 Alexander, S.P., Banner, F.T., 1984. The functional relationship between skeleton and cytoplasm in
362 *Haynesina germanica* (Ehrenberg). J. Foraminiferal Res. 14, 159-170.
363 Alve, E., Murray, J.W., 2001. Temporal variability in vertical distributions of live (stained) intertidal
364 foraminifera, Southern England. J. Foraminiferal Res. 31, 12-24.
365 Austin, H.A., Austin, W.E., Paterson, D.M., 2005. Extracellular cracking and content removal of the
366 benthic diatom *Pleurosigma angulatum* (Quekett) by the benthic foraminifera *Haynesina*
367 *germanica* (Ehrenberg). Mar. Micropaleontol. 57, 68-73.
368 Bedoshvili, Y.D., Popkova, T.P., Likhoshway, Y.V., 2009. Chloroplast structure of diatoms of
369 different classes. Cell Tissue Biol. 3, 297-310.
370 Bernhard, J.M., Alve, E., 1996. Survival, ATP pool, and ultrastructural characterization of benthic
371 foraminifera from Drammens fjord (Norway): Response to anoxia. Mar. Micropaleontol. 28, 5-
372 17.
373 Bernhard, J.M., Bowser, S.S., 1999. Benthic foraminifera of dysoxic sediments: chloroplast
374 sequestration and functional morphology. Earth Sci. Rev. 46, 149-165.
375 Bernhard, J.M., Buck, K.R., Farmer, M.A., Bowser, S.S., 2000. The Santa Barbara Basin is a
376 symbiosis oasis. Nature 403, 77-80.
377 Bouchet, V.M.P., Sauriau, P.G., Debenay, J.P., Mermillod-Blondin, F., Schmidt, S., Amiard, J.C.,
378 Dupas, B., 2009. Influence of the mode of macrofauna-mediated bioturbation on the vertical
379 distribution of living benthic foraminifera: First insight from axial tomodensitometry. J. Exp.
380 Mar. Biol. Ecol. 371, 20-33.

Cartaxana, P., Ruivo, M., Hubas, C., Davidson, I., Serôdio, J., Jesus, B., 2011. Physiological versus behavioral photoprotection in intertidal epipelic and epipsammic benthic diatom communities. J. Exp. Mar. Biol. Ecol. 405, 120-127.

Cedhagen, T., 1991. Retention of chloroplasts and bathymetric distribution in the sublittoral foraminiferan *Nonionellina labradorica*. Ophelia 33, 17-30.

Cesbron, F., Geslin, E., Jorissen, F.J., Delgard, M.L., Charrieau, L., Deflandre, B., Jézéquel, D., Anschutz, P., Metzger, E., 2016. Vertical distribution and respiration rates of benthic foraminifera: Contribution to aerobic remineralization in intertidal mudflats covered by *Zostera noltei* meadows. Estuar. Coast. Shelf Sci., 179, 23-38.

Cesbron, F., Geslin, E., Le Kieffre, C., Jauffrais, T., Nardelli, M.P., Langlet, D., Mabilleau, G., Jorissen, F., Jézéquel, D., Metzger, E., 2017. Sequestered chloroplasts in the benthic foraminifer *Haynesina germanica*: cellular organization, oxygen fluxes and potential ecological implications. J.Foraminiferal Res. 47, 268-278..

Clark, K.B., Jensen, K.R., Stirts, H.M., 1990. Survey for functional kleptoplasty among West Atlantic Ascoglossa (=Sacoglossa) (Mollusca: Opisthobranchia). Veliger 33, 339-345.

Correia, M.J., Lee, J.J., 2000. Chloroplast retention by *Elphidium excavatum* (Terquem). Is it a selective process? Symbiosis 29, 343-355.

Correia, M.J., Lee, J.J., 2002a. Fine structure of the plastids retained by the foraminifer *Elphidium excavatum* (Terquem). Symbiosis 32, 15-26.

Correia, M.J., Lee, J.J., 2002b. How long do the plastids retained by *Elphidium excavatum* (Terquem) last in their host? Symbiosis 32, 27-37.

Darling, K.F., Schweizer, M., Knudsen, K.L., Evans, K.M., Bird, C., Roberts, A., Filipsson, H.L., Kim, J.-H., Gudmundsson, G., Wade, C.M., Sayer, M.D.J., Austin, W.E.N., 2016. The genetic diversity, phylogeography and morphology of Elphidiidae (Foraminifera) in the Northeast Atlantic. Mar. Micropaleontol. 129, 1-23.

Debenay, J.-P., Guillou, J.-J., Redois, F., Geslin, E., 2000. Distribution trends of foraminiferal assemblages in paralic environments. A base for using foraminifera as bioindicators, in: Martin, R.E. (Ed.), Environmental Micropaleontology. Springer US, pp. 39-67.

409 Debenay, J.P., Bicchi, E., Goubert, E., du Chatelet, E.A., 2006. Spatio-temporal distribution of benthic
410 foraminifera in relation to estuarine dynamics (Vie estuary, Vendee, W France). Estuar. Coast.
411 Shelf Sci. 67, 181-197.
412 Goldstein, S.T., Bernhard, J.M., Richardson, E.A., 2004. Chloroplast sequestration in the foraminifer
413 *Haynesina germanica*: Application of high pressure freezing and freeze substitution. Microsc.
414 Microanal. 10, 1458-1459.
415 Gouy, M., Guindon, S., Gascuel, O., 2010. Sea view version 4: A multiplatform graphical user
416 interface for sequence alignment and phylogenetic tree building. Mol. Biol. Evol. 27, 221-224.
417 Grzymski, J., Schofield, O.M., Falkowski, P.G., Bernhard, J.M., 2002. The function of plastids in the
418 deep-sea benthic foraminifer, *Nonionella stella*. Limnol. Oceanogr. 47, 1569-1580.
419 Hayward, B.W., Holzmann, M., Grenfell, H.R., Pawlowski, J., Triggs, C.M., 2004. Morphological
420 distinction of molecular types in *Ammonia* - Towards a taxonomic revision of the world's most
421 commonly misidentified foraminifera. Mar. Micropaleontol. 50, 237-271.
422 Holzmann, M. and Pawlowski, J., 2017. An updated classification of rotaliid foraminifera based on
423 ribosomal DNA phylogeny. Mar. Micropaleontol.132, 18-34.
424 Horton, B.P., Edwards, R.J., 2006. Quantifying holocene sea level change using intertidal
425 foraminifera: Lessons from the British isles. Cushman Foundation for Foraminiferal Research,
426 Special Publication.
427 Jauffrais, T., Jesus, B., Geslin, E., Briand, F., Martin-Jézéquel, V., 2016a. Locomotion speed of the
428 benthic foraminifer *Ammonia tepida* exposed to different nitrogen and carbon sources. J. Sea
429 Res. 118, 52-58.
430 Jauffrais, T., Jesus, B., Méléder, V., Geslin, E., 2017. Functional xanthophyll cycle and pigment
431 content of a kleptoplastic benthic foraminifer: *Haynesina germanica*. PLoS ONE, 12, e0172678.
432 Jauffrais, T., Jesus, B., Metzger, E., Mouget, J.L., Jorissen, F., Geslin, E., 2016b. Effect of light on
433 photosynthetic efficiency of sequestered chloroplasts in intertidal benthic foraminifera
434 (*Haynesina germanica* and *Ammonia tepida*). Biogeosciences 13, 2715-2726.

435 Kitazato, H., 1988. Ecology of benthic foraminifera in the tidal zone of a rocky shore. Rev. Paléobiol.
436 Special publication 2, 815-825.
437 Kitazato, H., 1994. Foraminiferal microhabitats in four marine environments around Japan. Mar.
438 Micropaleontol. 24, 29-41.
439 Knight, R., Mantoura, R.F.C., 1985. Chlorophyll and carotenoid pigments in foraminifera and their
440 symbiotic algae: analysis by high performance liquid chromatography Mar. Ecol. Prog. Ser. 23,
441 241-249.
442 Koho, K.A., Piña-Ochoa, E., Geslin, E., Risgaard-Petersen, N., 2011. Vertical migration, nitrate
443 uptake and denitrification: survival mechanisms of foraminifers (*Globobulimina turgida*) under
444 low oxygen conditions. FEMS Microbiol. Ecol. 75, 273-283.
445 Kuhl, M., Lassen, C., Jorgensen, B.B., 1994. Light penetration and light-intensity in sandy marine-
446 sediments measured with irradiance and scalar irradiance fiberoptic microprobes. Mar. Ecol.
447 Prog. Ser. 105, 139-148.
448 Lee, J.J., Lanners, E., Ter Kuile, B., 1988. The retention of chloroplasts by the foraminifera *Elphidium*
449 *crispum*. Symbiosis 5, 45-60.
450 Leutenegger, S., 1977. Ultrastructure de foraminifères perforés et imperforés ainsi que de leurs
451 symbiotes. Cahiers de Micropaleontol. 3, 1-161.
452 Lopez, E., 1979. Algal chloroplasts in the protoplasm of three species of benthic foraminifera:
453 taxonomic affinity, viability and persistence. Mar. Biol. 53, 201-211.
454 Morvan, J., Debenay, J.P., Jorissen, F., Redois, F., Bénéteau, E., Delplancke, M., Amato, A.S., 2006.
455 Patchiness and life cycle of intertidal foraminifera: Implication for environmental and
456 paleoenvironmental interpretation. Mar. Micropaleontol. 61, 131-154.
457 Murray, J.W., 1991. Ecology and palaeoecology of benthic foraminifera. Longman, New York.
458 Pascal, P.Y., Dupuy, C., Richard, P., Mallet, C., du Chatelet, E.A., Niquil, N., 2009. Seasonal
459 variation in consumption of benthic bacteria by meio- and macrofauna in an intertidal mudflat.
460 Limnol. Oceanogr. 54, 1048-1059.
461 Pawlowski, J., 2000. Introduction to the molecular systematics of foraminifera. Micropaleontol. 46, 1-
462 12.

463 Pawlowski, J., Holzmann, M., 2014. A plea for DNA barcoding of foraminifera. J. Foraminiferal Res.
464 44, 62-67.
465 Pillet, L., de Vargas, C., Pawlowski, J., 2011. Molecular identification of sequestered diatom
466 chloroplasts and kleptoplastidy in foraminifera. Protist 162, 394-404.
467 Pillet, L., Voltski, I., Korsun, S., Pawlowski, J., 2013. Molecular phylogeny of Elphidiidae
468 (foraminifera). Mar. Micropaleontol. 103, 1-14.
469 Roberts, A., Austin, W., Evans, K., Bird, C., Schweizer, M., Darling, K., 2016. A new integrated
470 approach to taxonomy: The fusion of molecular and morphological systematics with type
471 material in benthic foraminifera. PLoS ONE 11, doi:10.1371/journal.pone.0158754.
472 Schmaljohann, R., Röttger, R., 1978. The ultrastructure and taxonomic identity of the symbiotic algae
473 of *Heterostegina depressa* (Foraminifera: Nummulitidae). J. Mar. Biol. Assoc. U. K. 58, 227-
474 237.
475 Schweizer, M., Pawlowski, J., Kouwenhoven, T.J., Guiard, J., van der Zwaan, B., 2008. Molecular
476 phylogeny of Rotaliida (Foraminifera) based on complete small subunit rDNA sequences. Mar.
477 Micropaleontol. 66, 233-246.
478 Schweizer, M., Polovodova, I., Nikulina, A., Schonfeld, J., 2011. Molecular identification of *Ammonia*
479 and *Elphidium* species (Foraminifera, Rotaliida) from the Kiel Fjord (SW Baltic Sea) with
480 rDNA sequences. Helgoland Mar. Res. 65, 1-10.
481 Thibault de Chanvalon, A., Metzger, E., Mouret, A., Cesbron, F., Knoery, J., Rozuel, E., Launeau, P.,
482 Nardelli, M.P., Jorissen, F.J., Geslin, E., 2015. Two-dimensional distribution of living benthic
483 foraminifera in anoxic sediment layers of an estuarine mudflat (Loire estuary, France).
484 Biogeosciences 12, 6219-6234.
485 Tsuchiya, M., Kitazato, H., Pawlowski, J., 2000. Phylogenetic relationships among species of
486 glabratellidae (foraminifera) inferred from ribosomal DNA sequences: Comparison with
487 morphological and reproductive data. Micropaleontol. 46, 13-20.
488 Tsuchiya, M., Kitazato, H., Pawlowski, J., 2003. Analysis of internal transcribed spacer of ribosomal
489 DNA reveals cryptic speciation in *Planoglabratella opercularis*. J. Foraminiferal Res. 33, 285-
490 293.

Tsuchiya, M., Takahara, K., Aizawa, M., Suzuki-Kanesaki, H., Toyofuku, T., Kitazato, H., 2014. How has foraminiferal genetic diversity developed? A case study of *Planoglabratella opercularis* and the species concept inferred from its ecology, distribution, genetics, and breeding behavior, in: Kitazato, H., Bernhard, J.M. (Eds.), Approaches to study living foraminifera: Collection, maintenance and experimentation. Springer Japan, Tokyo, pp. 133-162.

Tsuchiya, M., Toyofuku, T., Uematsu, K., Brüchert, V., Collen, J., Yamamoto, H., Kitazato, H., 2015. Cytologic and genetic characteristics of endobiotic bacteria and kleptoplasts of *Virgulinella fragilis* (Foraminifera). J. Euk. Microbiol. 62, 454-469.

Ultrastructure and distribution of kleptoplasts in benthic foraminifera from shallow-water (photic) habitats

Thierry Jauffrais[1*], Charlotte LeKieffre[2], Karoliina A. Koho[3], Masashi Tsuchiya[4], Magali Schweizer[1], Joan M. Bernhard[5], Anders Meibom[2,6], Emmanuelle Geslin[1]

[1] UMR CNRS 6112 LPG-BIAF, Bio-Indicateurs Actuels et Fossiles, Université d'Angers, 2 Boulevard Lavoisier, 49045 Angers CEDEX 1, France

[2] Laboratory for Biological Geochemistry, School of Architecture, Civil and Environmental Engineering (ENAC), Ecole Polytechnique Fédérale de Lausanne (EPFL), 1015 Lausanne, Switzerland

[3] University of Helsinki, Department of Environmental Sciences, Viikinkaari 1, Helsinki, Finland

[4] Department of Marine Biodiversity Research, Japan Agency for Marine-Earth Science and Technology, 2-15 Natsushima-cho, Yokosuka, Kanagawa, Japan

[5] Woods Hole Oceanographic Institution, Geology & Geophysics Department, Woods Hole, MA, USA

[6] Center for Advanced Surface Analysis, Institute of Earth Sciences, University of Lausanne, Switzerland

*contact: Thierry.jauffrais@univ-angers.fr

Abstract

Assimilation, sequestration and maintenance of foreign chloroplasts inside an organism is termed "chloroplast sequestration" or "kleptoplasty". This phenomenon is known in certain benthic foraminifera, in which such kleptoplasts can be found both intact and functional, but with different retention times depending on foraminiferal species. In the present study, seven species of benthic foraminifera (*Haynesina germanica*, *Elphidium williamsoni*, *E. selseyense*, *E. oceanense*, *E.* aff. *E. crispum*, *Planoglabratella opercularis* and *Ammonia* sp.) were collected from shallow-water benthic habitats and examined with transmission electron microscope (TEM) for cellular ultrastructure to ascertain attributes of kleptoplasts. Results indicate that all these foraminiferal taxa actively obtain kleptoplasts but organized them differently within their endoplasm. In some species, the kleptoplasts were evenly distributed throughout the endoplasm (e.g., *H. germanica*, *E. oceanense*, *Ammonia* sp.), whereas other species consistently had plastids distributed close to the external cell membrane (e.g., *Elphidium williamsoni*, *E. selseyense*, *P. opercularis*). Chloroplast degradation also seemed to differ between species, as many degraded plastids were found in *Ammonia* sp. and *E. oceanense* compared to other investigated species. Digestion ability, along with different feeding and sequestration strategies may explain the differences in retention time between taxa. Additionally, the organization of the sequestered plastids within the endoplasm may also suggest behavioral strategies to expose and/or protect the sequestered plastids to/from light and/or to favor gas and/or nutrient exchange with their surrounding habitats.

Key words

Kleptoplasty; protist; chloroplast; TEM; transmission electron microscope

548 **1. Introduction**

549 Some benthic foraminiferal species have the ability to steal and sequester chloroplasts (which then
550 become "kleptoplasts") from their microalgal food sources. These foraminiferal species mainly ingest
551 diatoms (Knight and Mantoura, 1985; Bernhard and Bowser 1999, Goldstein et al., 2004; Pillet et al.,
552 2011; Tsuchiya et al., 2015; Jauffrais et al., 2017) but have different strategies for feeding and
553 sequestration (Lopez, 1979; Grzymski et al., 2002; Austin et al., 2005; Jauffrais et al., 2016b). In some
554 foraminiferal species, the kleptoplasts are degraded within hours, possibly as a result of a digestive
555 process, while in other species they are kept and/or remain functional for weeks to months (Lopez,
556 1979; Lee et al., 1988; Cedhagen, 1991; Correia and Lee, 2000, 2002a, b; Grzymski et al., 2002;
557 Tsuchiya et al., 2015; Jauffrais et al., 2016b). A kleptoplast is thus a chloroplast, functional or not, that
558 was "stolen", integrated and sometimes used by a host organism (Clark et al., 1990). Benthic
559 foraminiferal kleptoplasty is observed in species from different environments: shallow to deep-sea,
560 oxic to anoxic and photic to aphotic habitats (Lopez, 1979; Alexander and Banner, 1984; Lee et al.,
561 1988; Bernhard and Alve, 1996; Bernhard and Bowser, 1999; Bernhard et al., 2000; Correia and Lee,
562 2000). The photosynthetic function of kleptoplasts has been demonstrated in some shallow-water
563 benthic foraminifera (e.g., *Elphidium williamsoni* and *Haynesina germanica* in Cesbron et al., 2017;
564 Jauffrais et al., 2016; Lopez, 1979). Nevertheless, it remains unknown why certain deep-sea
565 foraminifera sequester chloroplasts as light is absent in their habitat (Bernhard and Bowser, 1999;
566 Grzymski et al., 2002).

567 In photic shallow-water habitats (e.g., estuaries, bays, lagoons and other intertidal or shallow-water
568 subtidal areas), kleptoplastic benthic foraminiferal species, such as *Haynesina germanica, Elphidium*
569 *williamsoni,* the "*excavatum*" species complex (e.g., *E. oceanense*, *E. selseyense*, see Darling et al.
570 (2016)), or *Ammonia* spp., are often the dominant mudflat foraminiferal taxa (Debenay et al., 2000;
571 Debenay et al., 2006; Morvan et al., 2006; Bouchet et al., 2009; Pascal et al., 2009; Thibault de
572 Chanvalon et al., 2015; Cesbron et al., 2016). Their vertical distribution is characterized by a clear
573 maximum density in the upper oxygenated millimeters of the sediment (Alve and Murray, 2001;
574 Bouchet et al., 2009; Thibault de Chanvalon et al., 2015; Cesbron et al., 2016), where light can also
575 penetrate (Kuhl et al., 1994; Cartaxana et al., 2011). However, in some kleptoplastic species (e.g., the

morphospecies *A. tepida* and *E. excavatum*) kleptoplasts lack photosynthetic activity (Lopez, 1979; Jauffrais et al., 2016), and in many other kleptoplastic species, the photosynthetic activity has not yet been assessed and/or quantified.

The observed differences in the maintenance of the kleptoplasts suggest there must be substantial differences between kleptoplastic shallow-water foraminiferal species. It is, therefore, necessary to understand the sequestration mechanism in kleptoplastic foraminifera that have similar food sources and environments, but may have different chloroplast-retention times. In this study, we used transmission electron microscope (TEM) to document the ultrastructure and cellular organization of different kleptoplastic foraminifera from shallow-water photic habitats to assess chloroplast organization and degradation processes. In parallel, individuals from the same populations as the ultrastructurally examined specimens have been genetically characterized with DNA barcoding to ascertain their taxonomic identity to ease future comparisons.

2. Material and methods

2.1. Specimen collection and field sample fixations

We examined seven species of living shallow-water benthic foraminifera: *Haynesina germanica* (Fig. 1 and 2), *Elphidium williamsoni* (Fig. 3), *Elphidium oceanense* (Fig. 4), *Elphidium selseyense* (Fig. 5), *Elphidium* aff. *E. crispum* (Fig. 6), *Planoglabratella opercularis* (Fig. 7 and 8) and *Ammonia* sp. phylotype T6 (Fig. 9 and 10).

Haynesina germanica (4 specimens ultrathin sectioned and observed by TEM), *E. oceanense* (3 specimens ultrathin sectioned and observed by TEM) and *Ammonia* sp. (3 specimens ultrathin sectioned and observed by TEM) were collected from the Bourgneuf Bay tidal mudflat (Bay of Biscay, south of the Loire estuary, France), a 11 AM from surface sediments (~0-0.5 cm depth, temperature of the sediment 11°C, salinity 31) in March 2016 at low tide during a cloudy day. The foraminifera-bearing sediments were fixed in the field immediately after sampling, with a fixative solution containing 4% glutaraldehyde and 2% paraformaldehyde in artificial seawater (Red Sea® salt in MilliQ® water at salinity 35). The samples were then kept at room temperature (18-20°C) for 24 h and subsequently placed at 4°C until further processing.

Haynesina germanica (3 specimens ultrathin sectioned and observed by TEM) and *E. selseyense* (1 specimen ultrathin sectioned and observed by TEM) were isolated in February 2016 from two Wadden Sea tidal mudflats during low tide (Texel Island, the Netherlands): Mokbaai (sediment temperature = 4°C, salinity = 27, at 7:30AM on a sunny day) and Cocksdorp (sediment temperature = 4°C, salinity = 23, at 8AM on a sunny day). Sediment cores were sliced at 1-cm intervals down to 10-cm depth. The top 1-cm of each sediment core was sieved over a 125-µm screen and foraminifera containing healthy looking cytoplasm were picked within 30 h of sampling from the >125-µm fraction under illuminated binocular microscope. The vitality of all isolated foraminifera was further assessed based on movements as outlined in Koho et al. (2011). Immediately after vitality checks, living specimens were transferred to a fixative solution containing 2% glutaraldehyde and 4% paraformaldehyde in filtered seawater and stored at 4°C. After 24 h, the specimens were transferred into a solution containing 4% paraformaldehyde in filtered seawater and stored at 4°C, where they remained until further processing.

Elphidium williamsoni (5 specimens ultrathin sectioned and observed by TEM) were collected from surface sediments (0-0.5 cm depth) in May 2016 from a small tidal mudflat at low tide 2 PM, on a sunny day in Fiskebäckskil near Kristineberg Marine Research Station (Gullmar Fjord, Sweden). The sediments with foraminifera were fixed and preserved immediately in the field as noted for *H. germanica* from the Bourgneuf Bay tidal mudflat.

Elphidium aff. *E. crispum* (12 specimens ultrathin sectioned and observed by TEM) and *P. opercularis* (12 specimens ultrathin sectioned and observed by TEM) were isolated from coralline algae (*Corallina pilulifera*, Rhodophyta) collected from rocky shores of Yugawara (Kanagawa Prefecture, Japan) in May 2012 at 1 m depth. The vitality of all isolated foraminifera was assessed based on pseudopodial extension using an inverted microscope with a phase-contrast apparatus. Living specimens were picked with a fine (soft) needle, fixed for 2 h in 2.5% seawater-buffered glutaraldehyde and then transferred in filtered (0.2 µm) seawater and kept at 4°C until processing.

2.2. Species identifications

630 Specimens were taxonomically identified based solely on the morphology of the test as revealed with
631 a scanning electron microscope (SEM) or based on both morphology (SEM micrographs) and
632 molecular (DNA barcoding; DNA sequences) tools.
633 For the Bay of Bourgneuf and the Gullmar Fjord, foraminifera from the same sampling of specimens
634 used for the TEM studies were selected for DNA barcoding (Table 1). Live foraminifera were picked
635 from the sediment, dried on micropaleontological slides, imaged with an environmental SEM (EVO
636 LS10, ZEISS) and individually extracted for DNA in Deoxycholate (DOC) buffer (e.g., Pawlowski,
637 2000; Schweizer et al., 2011). For the DNA amplification, a fragment situated at the 3' end of the
638 small subunit (SSU) rDNA was selected because this region is the barcode for foraminifera
639 (Pawlowski and Holzmann, 2014). The primer pairs were s14F3 and J2 for the primary polymerase
640 chain reactions (PCR) and s14F1 and N6 for the secondary (nested) PCR (Pawlowski, 2000; Darling et
641 al., 2016). Positive PCR gave a fragment of about 500 nucleotides (nt) that was purified and
642 sequenced directly as described in Schweizer et al. (2011).
643 New DNA sequences were deposited in GenBank (accession numbers KY347797-KY347800).
644 For the Dutch and Japanese specimens, available DNA sequences (Schweizer et al., 2008; Schweizer
645 et al., 2011; Tsuchiya et al., 2000; Pawlowski and Holzmann, unpublished data) were gathered from
646 GenBank (Table 1).
647 The sequences retrieved from the studied species (Table 1) were then compared to published
648 sequences (Hayward et al., 2004; Darling et al., 2016) within an alignment obtained with SeaView
649 (Gouy et al., 2010) to identify them molecularly.
650
651 *2.3. Ultrastructural observations by TEM*
652 Chemically preserved specimens were rinsed in filtered seawater and then either decalcified in 0.1 or
653 0.5 M ethylenediamine tetraacetic acid (EDTA) prepared in distilled water (pH 7.4) and post-fixed
654 with 2% osmium tetroxide (OsO_4) solution prepared in filtered seawater for about 1-2 h, or the reverse
655 (both processes worked). Foraminifera were then dehydrated with successive ethanol baths and
656 embedded in resin, either Epon (Epon 812 resin, TAAB) or LR White® (Sigma-Aldrich). Ultra-thin
657 sections (60-70 nm) were prepared with an ultra-microtome (Reichert Ultracut S, Leica) after staining

658 with uranyl acetate, or with 1% aqueous uranyl acetate and 0.5% lead citrate, and then coated with
659 carbon using a JEE-400 high vacuum evaporator (JEOL Ltd). The ultrathin sections were finally
660 examined with either a JEM-1400 (JEOL Ltd), JEM-1210 (JEOL Ltd) or TECNAI G2 20 (FEI
661 Company) TEM at an acceleration voltage of 80-100kV.
662
663 **3. Results and discussion**
664 This contribution presents the ultrastructure and cellular distribution of kleptoplasts, highlighting
665 differences in chloroplast organization and degradation processes in foraminifera from shallow-water
666 habitats (synopsis in Table 2). The description and organization of other organelles in benthic
667 foraminifera are described in detail elsewhere (see, LeKieffre et al., this issue).
668
669 *3.1. Haynesina germanica* (Fig. 1 and 2)
670 *Haynesina germanica* is relatively easy to recognize morphologically and there is good congruence
671 between morphological and molecular identification (Darling et al., 2016, phylotype S16);
672 consistently, we found good agreement between the molecular and morphological identification of the
673 specimens collected from the Bourgneuf Bay tidal mudflat (France). Direct molecular identification
674 was not performed on specimens collected from Texel (Mokbaai, NL). However, specimens from a
675 nearby site (Wadden Sea, Den Oever, NL) that were sequenced and identified as phylotype S16
676 (Schweizer et al., 2011, Table 1) bore similar morphology to Mokbaai specimens.
677 In all four specimens studied with TEM, the kleptoplasts were evenly distributed in each chamber and
678 large vacuoles were also densely and evenly distributed (Fig. 1B, C and Fig. 2B). The chloroplasts
679 showed fine structural details and were relatively well preserved in the foraminiferal endoplasm with
680 thylakoids, girdle lamella surrounding each kleptoplast and pyrenoids (Fig. 1E, F, and Fig. 2C, E). The
681 pyrenoids were also well preserved, often transected by a lamella and surrounded by another lamella
682 (Fig. 1E, F and Fig. 2C, E). Ideally in *H. germanica*, five membranes are visible around the
683 chloroplast; the four inner membranes are most likely those of the diatom and the fifth and outermost
684 membrane is that of the foraminifer (Goldstein et al., 2004). In the present study, an electron-lucent
685 space was often observed between the chloroplast membranes and the host membrane (Fig. 1 D, E and

686 F, and Fig. 2E). This electron-lucent space may be an artefact caused by the chemical fixation and
687 embedding procedures.
688
689 *3.2. Elphidium williamsoni* (Fig. 3)
690 The morphospecies *Elphidium williamsoni* has been formally linked to phylotype S1 (Darling et al.,
691 2016) with DNA sequencing of topotypic specimens (Roberts et al., 2016). A specimen from the
692 Gullmar Fjord sample was also sequenced and found to belong to phylotype S1 (Table 1), confirming
693 the morphological determination.
694 Kleptoplasts were abundant and situated just below the cell periphery (Fig. 3B, C) or close to it (Fig.
695 3D). Kleptoplasts were also well preserved with pyrenoid, lamella and thylakoids (Fig. 3E, F). A
696 degraded kleptoplast at the foraminiferal cell periphery had inter-thylakoid spaces (Fig. 3C (c*)). As
697 observed in *H. germanica,* the kleptoplasts were surrounded by host membrane, with electron-lucent
698 spaces between the chloroplasts and the endoplasm of the host (Fig. 3B to F) that may be an artefact
699 caused by the chemical fixation and embedding procedures.
700
701 *3.3. Elphidium "excavatum"* species complex (Fig. 4 and 5)
702 *Elphidium oceanense* and *E. selseyense* belong to the "*excavatum*" species complex as defined by
703 Darling et al. (2016). The morphospecies *Elphidium excavatum* was thought to include a large number
704 of ecophenotypes due to its high morphological diversity. However, recent molecular phylogenetics
705 studies have shown that this morphospecies is actually a species complex (Schweizer et al., 2011;
706 Pillet et al., 2013; Darling et al., 2016). These species are pseudocryptic, meaning that a careful
707 morphological examination of specimens traditionally determined as *E. excavatum* allows
708 classification to one species of the complex (Darling et al., 2016). Presently, four different phylotypes
709 have been identified and linked to previously described morphological forms that were then given
710 species status: S3=*E. oceanense*, S4=*E. clavatum*, S5=*E. selseyense*, S13=*E. lidoense* (Darling et al.,
711 2016).
712
713 3.3.1. *Elphidium oceanense* (Fig. 4)

714 Specimens collected from the Bourgneuf Bay tidal mudflat, France, were morphologically and
715 molecularly identified as phylotype S3 in Darling et al. (2016). This phylotype is the most common
716 member of the "*excavatum*" species complex in the Bourgneuf Bay tidal mudflat (Schweizer et al.,
717 unpublished results and Table 1).
718 In *E. oceanense,* kleptoplasts and vacuoles were evenly and densely distributed in the endoplasm (Fig.
719 4C, D). The kleptoplasts were in large vacuoles containing numerous plastids and fine materials (Fig.
720 4D - F). The plastids often appeared in a degraded state with small circular electron-lucent disruptions
721 of thylakoids and pyrenoids (Fig. 4E, F). Kleptoplast pyrenoids, lamella and thylakoids remained
722 clearly distinguishable (Fig. 4E, F).
723
724 3.3.2. *Elphidium selseyense* (Fig. 5)
725 The specimens from Cocksdorp (Wadden Sea) were identified morphologically as *E. selseyense.* This
726 species, which is linked to the phylotype S5 (Darling et al., 2016), was isolated in 1999 from the same
727 location (Schweizer et al., 2011; Table 1). *Elphidium selseyense* is known as a widespread and
728 opportunistic species with ecology similar to the other species described above (Murray, 1991; Horton
729 and Edwards, 2006; Darling et al., 2016).
730 Specimens of *E. selseyense* had many kleptoplasts situated immediately below the host-cell periphery
731 (Fig. 5B, C and D) with relatively fewer chloroplasts internally in the endoplasm (Fig. 5B).
732 Kleptoplasts exhibited a girdle lamella, a simple pyrenoid, thylakoids and also osmiophilic globules
733 (Bedoshvili et al., 2009), which could be lipoprotein particles such as plastoglobules as suggested
734 previously by Leutenegger (1977) and Schmaljohann and Röttger (1978).
735 Despite being phylogenetically closely related (Darling et al. 2016), *E. oceanense* and *E. selseyense*
736 clearly have different chloroplast sequestration strategies. First, the plastids were distributed
737 throughout cytoplasm in *E. oceanense* compared to *E. selseyense,* where the plastids occurred
738 peripherally. Second, the kleptoplasts were relatively degraded in *E. oceanense* and relatively intact in
739 *E. selseyense*. Third, multiple plastids occurred in one vacuole of *E. oceanense* whereas, typically, a
740 single plastid was seen in one vacuole of *E. selseyense*. These differences suggest that, in *E.*
741 *oceanense,* the kleptoplasts were not functional, whereas, in *E. selseyense* they may still be functional,

742 possibly producing oxygen and assimilating inorganic carbon and nitrogen. Although these two
743 *Elphidium* taxa are within the same species complex as defined by Darling et al. (2016), differences in
744 chloroplast maintenance and distribution reveal that the species differ not only genetically and
745 morphologically, but also physiologically. Such observations emphasize the need to clearly identify
746 individuals within this species complex. These differences within the same species complex also
747 hamper direct comparison with previous studies on *E. excavatum* structures (Lopez, 1979; Correia and
748 Lee, 2000, 2002a, b) where no morphological (SEM images) and/or molecular (sequence) data are
749 available.
750
751 *3.4. Elphidium* aff. *E. crispum* (Fig. 6)
752 Specimens of *E.* aff. *E. crispum* were isolated from intertidal rocky shores of Yugawara (Kanagawa
753 Prefecture, Japan) where they are commonly encountered living on coralline algae (Kitazato, 1994).
754 No published sequence data is yet available for this species, but the preliminary analysis of the
755 sequences differs from the European *E. crispum* (phylotype S11, Darling et al., 2016 and Tsuchiya,
756 unpubl. data), therefore explaining the use of open nomenclature here.
757 Kleptoplasts were evenly and densely distributed in the endoplasm (Fig. 6B, C, F). Some organelles
758 such as mitochondria, Golgi apparatus, and peroxisomes were found near the kleptoplasts (Fig. 6D).
759 The kleptoplasts appear singly in vacuoles and have a girdle lamella, thylakoids, and pyrenoid divided
760 in two by a lamella and the presence of osmiophilic globules (Fig. 6E and G). Kleptoplasts were noted
761 in different states of degradation (Fig. 6H).
762
763 *3.5. Planoglabratella opercularis* (Fig. 7 and 8)
764 *Planoglabratella opercularis* is also commonly encountered in the intertidal zone of rocky shores
765 around the Japanese Islands where it lives on thalli of coralline algae (Kitazato, 1988; Tsuchiya et al.,
766 2014). Specimens collected near the TEM-sample collection site have been sequenced previously for
767 the large subunit (LSU) and SSU rDNA (Tsuchiya et al., 2000 see Table 1) and Internal transcribed
768 spacer (ITS) rDNA sequences (Tsuchiya et al., 2003; Tsuchiya et al., 2014, see Table 1). Moreover,
769 SSU rDNA sequences of *P. opercularis* from China have now been deposited in GenBank

(LN714815-LN714825; Holzmann and Pawlowski, 2017). The LSU rDNA sequence of a deposited Chinese specimen is identical to LSU sequences of the Japanese *P. opercularis* (Table 1).

Because *P. opercularis* is trochospiral with an attached mobile mode of life and directly exposed to sunlight, chloroplast distribution and sequestration are discussed in the context of spiral, umbilical and lateral perspectives, respectively (Fig. 7A-C). Kleptoplasts were situated at the proximity of the foraminifer's spiral surface, close to the pores and pores plates, where they formed a continuous layer of chloroplasts (Fig. 7B and Fig.8A, B). Also, some of the plastids were distributed in the endoplasm but at a lower density (Fig. 7B, 8E). Surrounding organelles such as mitochondria and Golgi apparatus were also found close to the kleptoplasts (Fig. 7F). The kleptoplasts were well preserved with thylakoids and a pyrenoid (Fig. 7C, D, F). Such peripheral distributions suggest active strategies of *P. opercularis* to maximise light acquisition by the kleptoplast, to favor gas (e.g., O_2, CO_2) and/or dissolved nutrient (e.g., nitrogen) exchanges with their surrounding habitats.

3.6. Ammonia sp. (phylotype T6, Fig. 9 and 10)

Ammonia isolated in Bourgneuf Bay tidal mudflat (France) were first identified as the morphospecies *A. tepida* (Jauffrais et al., 2016a). This morphospecies, however, is polyphyletic, with morphologically identical specimens belonging to distantly related species genetically (Hayward et al., 2004). Specimens from the same sample as the TEM-studied ones were sequenced (Schweizer et al., unpublished results and Table 1) and identified as *Ammonia* sp. (phylotype T6, Hayward et al., 2004).

Kleptoplasts were evenly distributed through chambers, along with diatom frustules and large vacuoles (Fig. 9B). An entire section of a diatom was noted in the endoplasm of one host (Fig. 9D). In this case, the degradation of the diatom had begun because the diatom cell had shrunken within the frustule, however, the detailed intracellular organization of the diatom remained clearly visible. Two chloroplasts with a simple pyrenoid were observable; they were linked by a bridge of cytoplasm where a nucleus and small vacuoles were also visible. A thin layer of cytoplasm then extended to the ends of the cell surrounding two large vacuoles and mitochondria.

Kleptoplasts of *Ammonia* sp. appeared in different states of degradation (Fig. 10). In well-preserved kleptoplasts, the pyrenoid was separated by a lamella composed of a thylakoid and surrounded by an

798 electron-lucent lamella (Fig. 10A). The thylakoids and girdle lamella were also visible (Fig. 10A and
799 B). In degraded kleptoplasts, the structure of the thylakoids and pyrenoid was disrupted and the
800 lamellae were degraded. These degraded kleptoplasts had inter-thylakoid spaces (Fig. 10C and D).
801 Their degradation state and the fact that *Ammonia* sp. kleptoplasts are known to quickly become non-
802 functional (Jauffrais et al., 2016b) suggest that this species merely feeds on diatoms and does not
803 sequester chloroplasts to perform photosynthesis.
804
805 *3.7. General discussion*
806 Our findings indicate that all seven foraminiferal taxa studied actively sequester chloroplasts but
807 sequestration strategies differed between species.
808 Firstly, the structure of the pyrenoid (one transecting lamella surrounded by one membrane), the
809 presence of a girdle lamella and, thylakoids, and the absence of starch accumulation, together other
810 evidence (ultrastructural, pigment and molecular analyses of the sequestered plastids, Goldstein et al.,
811 2004; Knight and Mantoura, 1985; Pillet et al., 2011, Jauffrais et al. 2016), suggest that the
812 kleptoplasts in all seven species belonged to diatoms. Similar ultrastructural, pigment and molecular
813 analyses confirm a similar source for deep-water kleptoplastic benthic foraminifera (Bernhard and
814 Bowser 1999; Grzymski et al., 2001). Secondly, kleptoplast distributions within the endoplasm
815 differed. In some species, the kleptoplasts were evenly distributed (e.g., *H. germanica*, *E. oceanense*
816 and *Ammonia* sp.), whereas in other species the plastids were located close to the cell periphery (e.g.,
817 *E. williamsoni*, *E. selseyense*, *P. opercularis*) and pore-plate complexes (e.g., *P. opercularis*). The
818 differences in the organization of plastids within the endoplasm suggest different behavioral strategies,
819 which expose and/or protect the sequestered plastids to/from light, and can favor gas (e.g., O_2, CO_2)
820 and dissolved nutrient (e.g., ammonium, nitrate) exchange with their surrounding habitats. Peripheral
821 chloroplast distributions might be considered as an active strategy of the foraminifer (e.g., *E.*
822 *williamsoni*, *E. selseyense*, *P. opercularis*) to maximize light acquisition by kleptoplasts. In contrast,
823 an internal distribution of kleptoplasts (e.g., *H. germanica*, *E. oceanense* and *Ammonia* sp.) could be
824 considered either as an absence of strategy, as a strategy to protect the kleptoplasts from an excess of
825 light and/or as an alternative strategy to maximize light exposure by continuously moving kleptoplasts

826 in the endoplasm of the cell to modulate light exposure. These results emphasize that studies on
827 kleptoplast ultrastructure of benthic foraminifera must be interpreted with care, as results on their
828 distribution might be influenced by the foraminiferal light exposure in the field and/or during
829 experimental studies. Contrary to the present study were the ambient light intensity before fixation is
830 unknown. We thus recommend for future ultrastructural studies to include control, or measure of light
831 intensity. In any case, the clear difference in the chloroplast organization between two
832 phylogenetically closely related species, *E. oceanense* and *E. selseyense* (Darling et al., 2016), lends a
833 novel (physiological) attribute distinguishing the two species beyond genetics and morphology.
834 Thirdly, chloroplast degradation timescale and the processes involved seem to be species specific as
835 many degraded plastids were found in *E. oceanense* and *Ammonia* sp. compared to other species.
836 Furthermore, the presence of numerous degraded chloroplasts in the endoplasm of *Ammonia* sp. and *E.*
837 *oceanense* is consistent with the absence of photosynthetic activity in both of these species (Lopez,
838 1979; Jauffrais et al., 2016b).
839 Finally, ingestion and sequestration strategies also differed among taxa. Diatom frustules were only
840 found in *Ammonia* sp. while other species had isolated plastids lacking frustules. Another
841 distinguishing characteristic could be the number of sequestered plastids (single to multiple)
842 surrounded by a single host membrane. Such variations may be related to differences in chloroplast
843 maintenance between foraminiferal species.
844

845 **Acknowledgements**

846 The authors thank Romain Mallet, Florence Manero, and Guillaume Mabilleau for their help at the
847 Imaging core facility (SCIAM laboratory) of the University of Angers, and Sophie Quinchard (UMR
848 6112 LPG-BIAF) for her technical help in the molecular identification of the different foraminiferal
849 species. TJ was funded by the "FRESCO" project, a project supported by the Region Pays de Loire
850 and the University of Angers. This work was also supported by a grant no. 200021_149333 from the
851 Swiss National Science Foundation and the French national program EC2CO-LEFE (project
852 ForChlo).JMB acknowledges the Robert W. Morse Chair for Excellence in Oceanography and the
853 Investment in Science Fund at WHOI. Also, KK acknowledges the Academy of Finland (Project

numbers: 278827, 283453), the electron Microscopy unit of University of Helsinki and the Netherlands Institute for Sea Research for funding, preparation and assistance with TEM and SEM images, and for providing facilities to conduct fieldwork in the Dutch Wadden Sea. MT thanks Katsuyuki Uematsu and Akihiro Tame (Marine Works Japan, Ltd) for their help with TEM preparations. The authors would like to thank Prof Richard Jordan for editing this article.

References

Alexander, S.P., Banner, F.T., 1984. The functional relationship between skeleton and cytoplasm in *Haynesina germanica* (Ehrenberg). J. Foraminiferal Res. 14, 159-170.

Alve, E., Murray, J.W., 2001. Temporal variability in vertical distributions of live (stained) intertidal foraminifera, Southern England. J. Foraminiferal Res. 31, 12-24.

Austin, H.A., Austin, W.E., Paterson, D.M., 2005. Extracellular cracking and content removal of the benthic diatom *Pleurosigma angulatum* (Quekett) by the benthic foraminifera *Haynesina germanica* (Ehrenberg). Mar. Micropaleontol. 57, 68-73.

Bedoshvili, Y.D., Popkova, T.P., Likhoshway, Y.V., 2009. Chloroplast structure of diatoms of different classes. Cell Tissue Biol. 3, 297-310.

Bernhard, J.M., Alve, E., 1996. Survival, ATP pool, and ultrastructural characterization of benthic foraminifera from Drammens fjord (Norway): Response to anoxia. Mar. Micropaleontol. 28, 5-17.

Bernhard, J.M., Bowser, S.S., 1999. Benthic foraminifera of dysoxic sediments: chloroplast sequestration and functional morphology. Earth Sci. Rev. 46, 149-165.

Bernhard, J.M., Buck, K.R., Farmer, M.A., Bowser, S.S., 2000. The Santa Barbara Basin is a symbiosis oasis. Nature 403, 77-80.

Bouchet, V.M.P., Sauriau, P.G., Debenay, J.P., Mermillod-Blondin, F., Schmidt, S., Amiard, J.C., Dupas, B., 2009. Influence of the mode of macrofauna-mediated bioturbation on the vertical distribution of living benthic foraminifera: First insight from axial tomodensitometry. J. Exp. Mar. Biol. Ecol. 371, 20-33.

881 Cartaxana, P., Ruivo, M., Hubas, C., Davidson, I., Serôdio, J., Jesus, B., 2011. Physiological versus
882 behavioral photoprotection in intertidal epipelic and epipsammic benthic diatom communities. J.
883 Exp. Mar. Biol. Ecol. 405, 120-127.
884 Cedhagen, T., 1991. Retention of chloroplasts and bathymetric distribution in the sublittoral
885 foraminiferan *Nonionellina labradorica*. Ophelia 33, 17-30.
886 Cesbron, F., Geslin, E., Jorissen, F.J., Delgard, M.L., Charrieau, L., Deflandre, B., Jézéquel, D.,
887 Anschutz, P., Metzger, E., 2016. Vertical distribution and respiration rates of benthic
888 foraminifera: Contribution to aerobic remineralization in intertidal mudflats covered by *Zostera*
889 *noltei* meadows. Estuar. Coast. Shelf Sci., 179, 23-38.
890 Cesbron, F., Geslin, E., Le Kieffre, C., Jauffrais, T., Nardelli, M.P., Langlet, D., Mabilleau, G.,
891 Jorissen, F., Jézéquel, D., Metzger, E., 2017. Sequestered chloroplasts in the benthic foraminifer
892 *Haynesina germanica*: cellular organization, oxygen fluxes and potential ecological
893 implications. J.Foraminiferal Res. 47, 268-278..
894 Clark, K.B., Jensen, K.R., Stirts, H.M., 1990. Survey for functional kleptoplasty among West Atlantic
895 Ascoglossa (=Sacoglossa) (Mollusca: Opisthobranchia). Veliger 33, 339-345.
896 Correia, M.J., Lee, J.J., 2000. Chloroplast retention by *Elphidium excavatum* (Terquem). Is it a
897 selective process? Symbiosis 29, 343-355.
898 Correia, M.J., Lee, J.J., 2002a. Fine structure of the plastids retained by the foraminifer *Elphidium*
899 *excavatum* (Terquem). Symbiosis 32, 15-26.
900 Correia, M.J., Lee, J.J., 2002b. How long do the plastids retained by *Elphidium excavatum* (Terquem)
901 last in their host? Symbiosis 32, 27-37.
902 Darling, K.F., Schweizer, M., Knudsen, K.L., Evans, K.M., Bird, C., Roberts, A., Filipsson, H.L.,
903 Kim, J.-H., Gudmundsson, G., Wade, C.M., Sayer, M.D.J., Austin, W.E.N., 2016. The genetic
904 diversity, phylogeography and morphology of Elphidiidae (Foraminifera) in the Northeast
905 Atlantic. Mar. Micropaleontol. 129, 1-23.
906 Debenay, J.-P., Guillou, J.-J., Redois, F., Geslin, E., 2000. Distribution trends of foraminiferal
907 assemblages in paralic environments. A base for using foraminifera as bioindicators, in: Martin,
908 R.E. (Ed.), Environmental Micropaleontology. Springer US, pp. 39-67.

909 Debenay, J.P., Bicchi, E., Goubert, E., du Chatelet, E.A., 2006. Spatio-temporal distribution of benthic
910 foraminifera in relation to estuarine dynamics (Vie estuary, Vendee, W France). Estuar. Coast.
911 Shelf Sci. 67, 181-197.
912 Goldstein, S.T., Bernhard, J.M., Richardson, E.A., 2004. Chloroplast sequestration in the foraminifer
913 *Haynesina germanica*: Application of high pressure freezing and freeze substitution. Microsc.
914 Microanal. 10, 1458-1459.
915 Gouy, M., Guindon, S., Gascuel, O., 2010. Sea view version 4: A multiplatform graphical user
916 interface for sequence alignment and phylogenetic tree building. Mol. Biol. Evol. 27, 221-224.
917 Grzymski, J., Schofield, O.M., Falkowski, P.G., Bernhard, J.M., 2002. The function of plastids in the
918 deep-sea benthic foraminifer, *Nonionella stella*. Limnol. Oceanogr. 47, 1569-1580.
919 Hayward, B.W., Holzmann, M., Grenfell, H.R., Pawlowski, J., Triggs, C.M., 2004. Morphological
920 distinction of molecular types in *Ammonia* - Towards a taxonomic revision of the world's most
921 commonly misidentified foraminifera. Mar. Micropaleontol. 50, 237-271.
922 Holzmann, M. and Pawlowski, J., 2017. An updated classification of rotaliid foraminifera based on
923 ribosomal DNA phylogeny. Mar. Micropaleontol.132, 18-34.
924 Horton, B.P., Edwards, R.J., 2006. Quantifying holocene sea level change using intertidal
925 foraminifera: Lessons from the British isles. Cushman Foundation for Foraminiferal Research,
926 Special Publication.
927 Jauffrais, T., Jesus, B., Geslin, E., Briand, F., Martin-Jézéquel, V., 2016a. Locomotion speed of the
928 benthic foraminifer *Ammonia tepida* exposed to different nitrogen and carbon sources. J. Sea
929 Res. 118, 52-58.
930 Jauffrais, T., Jesus, B., Méléder, V., Geslin, E., 2017. Functional xanthophyll cycle and pigment
931 content of a kleptoplastic benthic foraminifer: *Haynesina germanica*. PLoS ONE, 12, e0172678.
932 Jauffrais, T., Jesus, B., Metzger, E., Mouget, J.L., Jorissen, F., Geslin, E., 2016b. Effect of light on
933 photosynthetic efficiency of sequestered chloroplasts in intertidal benthic foraminifera
934 (*Haynesina germanica* and *Ammonia tepida*). Biogeosciences 13, 2715-2726.

935 Kitazato, H., 1988. Ecology of benthic foraminifera in the tidal zone of a rocky shore. Rev. Paléobiol.
936 Special publication 2, 815-825.
937 Kitazato, H., 1994. Foraminiferal microhabitats in four marine environments around Japan. Mar.
938 Micropaleontol. 24, 29-41.
939 Knight, R., Mantoura, R.F.C., 1985. Chlorophyll and carotenoid pigments in foraminifera and their
940 symbiotic algae: analysis by high performance liquid chromatography Mar. Ecol. Prog. Ser. 23,
941 241-249.
942 Koho, K.A., Piña-Ochoa, E., Geslin, E., Risgaard-Petersen, N., 2011. Vertical migration, nitrate
943 uptake and denitrification: survival mechanisms of foraminifers (*Globobulimina turgida*) under
944 low oxygen conditions. FEMS Microbiol. Ecol. 75, 273-283.
945 Kuhl, M., Lassen, C., Jorgensen, B.B., 1994. Light penetration and light-intensity in sandy marine-
946 sediments measured with irradiance and scalar irradiance fiberoptic microprobes. Mar. Ecol.
947 Prog. Ser. 105, 139-148.
948 Lee, J.J., Lanners, E., Ter Kuile, B., 1988. The retention of chloroplasts by the foraminifera *Elphidium*
949 *crispum*. Symbiosis 5, 45-60.
950 Leutenegger, S., 1977. Ultrastructure de foraminifères perforés et imperforés ainsi que de leurs
951 symbiotes. Cahiers de Micropaleontol. 3, 1-161.
952 Lopez, E., 1979. Algal chloroplasts in the protoplasm of three species of benthic foraminifera:
953 taxonomic affinity, viability and persistence. Mar. Biol. 53, 201-211.
954 Morvan, J., Debenay, J.P., Jorissen, F., Redois, F., Bénéteau, E., Delplancke, M., Amato, A.S., 2006.
955 Patchiness and life cycle of intertidal foraminifera: Implication for environmental and
956 paleoenvironmental interpretation. Mar. Micropaleontol. 61, 131-154.
957 Murray, J.W., 1991. Ecology and palaeoecology of benthic foraminifera. Longman, New York.
958 Pascal, P.Y., Dupuy, C., Richard, P., Mallet, C., du Chatelet, E.A., Niquil, N., 2009. Seasonal
959 variation in consumption of benthic bacteria by meio- and macrofauna in an intertidal mudflat.
960 Limnol. Oceanogr. 54, 1048-1059.
961 Pawlowski, J., 2000. Introduction to the molecular systematics of foraminifera. Micropaleontol. 46, 1-
962 12.

963 Pawlowski, J., Holzmann, M., 2014. A plea for DNA barcoding of foraminifera. J. Foraminiferal Res.
964 44, 62-67.
965 Pillet, L., de Vargas, C., Pawlowski, J., 2011. Molecular identification of sequestered diatom
966 chloroplasts and kleptoplastidy in foraminifera. Protist 162, 394-404.
967 Pillet, L., Voltski, I., Korsun, S., Pawlowski, J., 2013. Molecular phylogeny of Elphidiidae
968 (foraminifera). Mar. Micropaleontol. 103, 1-14.
969 Roberts, A., Austin, W., Evans, K., Bird, C., Schweizer, M., Darling, K., 2016. A new integrated
970 approach to taxonomy: The fusion of molecular and morphological systematics with type
971 material in benthic foraminifera. PLoS ONE 11, doi:10.1371/journal.pone.0158754.
972 Schmaljohann, R., Röttger, R., 1978. The ultrastructure and taxonomic identity of the symbiotic algae
973 of *Heterostegina depressa* (Foraminifera: Nummulitidae). J. Mar. Biol. Assoc. U. K. 58, 227-
974 237.
975 Schweizer, M., Pawlowski, J., Kouwenhoven, T.J., Guiard, J., van der Zwaan, B., 2008. Molecular
976 phylogeny of Rotaliida (Foraminifera) based on complete small subunit rDNA sequences. Mar.
977 Micropaleontol. 66, 233-246.
978 Schweizer, M., Polovodova, I., Nikulina, A., Schonfeld, J., 2011. Molecular identification of *Ammonia*
979 and *Elphidium* species (Foraminifera, Rotaliida) from the Kiel Fjord (SW Baltic Sea) with
980 rDNA sequences. Helgoland Mar. Res. 65, 1-10.
981 Thibault de Chanvalon, A., Metzger, E., Mouret, A., Cesbron, F., Knoery, J., Rozuel, E., Launeau, P.,
982 Nardelli, M.P., Jorissen, F.J., Geslin, E., 2015. Two-dimensional distribution of living benthic
983 foraminifera in anoxic sediment layers of an estuarine mudflat (Loire estuary, France).
984 Biogeosciences 12, 6219-6234.
985 Tsuchiya, M., Kitazato, H., Pawlowski, J., 2000. Phylogenetic relationships among species of
986 glabratellidae (foraminifera) inferred from ribosomal DNA sequences: Comparison with
987 morphological and reproductive data. Micropaleontol. 46, 13-20.
988 Tsuchiya, M., Kitazato, H., Pawlowski, J., 2003. Analysis of internal transcribed spacer of ribosomal
989 DNA reveals cryptic speciation in *Planoglabratella opercularis*. J. Foraminiferal Res. 33, 285-
990 293.

991 Tsuchiya, M., Takahara, K., Aizawa, M., Suzuki-Kanesaki, H., Toyofuku, T., Kitazato, H., 2014. How
992 has foraminiferal genetic diversity developed? A case study of *Planoglabratella opercularis* and
993 the species concept inferred from its ecology, distribution, genetics, and breeding behavior, in:
994 Kitazato, H., Bernhard, J.M. (Eds.), Approaches to study living foraminifera: Collection,
995 maintenance and experimentation. Springer Japan, Tokyo, pp. 133-162.
996 Tsuchiya, M., Toyofuku, T., Uematsu, K., Brüchert, V., Collen, J., Yamamoto, H., Kitazato, H., 2015.
997 Cytologic and genetic characteristics of endobiotic bacteria and kleptoplasts of *Virgulinella*
998 *fragilis* (Foraminifera). J. Euk. Microbiol. 62, 454-469.

Figure 1. *Haynesina germanica* (phylotype S16) isolated from Bourgneuf Bay (France). **A.** SEM. **B.** Light micrograph of semi-thin section showing vacuoles (v). **C-F**. TEM micrographs. **C.** Overview of a chamber showing kleptoplasts (c) and digestive vacuoles (dv) evenly and densely distributed in the endoplasm. **D and E.** Kleptoplast with thylakoid (th), girdle lamella (gl); pyrenoids (py). **F.** Higher magnification view of a kleptoplast with the girdle lamella (gl) surrounding the kleptoplast, thylakoids (th), a pyrenoid (py) with a lamella (la) inside and a lamella surrounding the pyrenoid (lp). **Scale bars:** A, B = 50 µm, C = 20 µm, D = 2 µm, E = 1µm and F = 0.5 µm.

Figure 2. *Haynesina germanica* (phylotype S16) isolated from Wadden Sea (Texel, Netherlands). **A.** Scanning electron micrograph. **B-E.** TEM micrographs. **B.** Overview of a chamber showing kleptoplasts (c) and vacuoles (v) evenly and densely distributed in the endoplasm. **C - E.** Kleptoplasts with pyrenoid (py), thylakoids (th) and osmiophilic globules (possibly plastoglobules). **Scale bars:** A= 100 µm, B = 5µm, C and D = 0.5 µm and E = 1µm.

Figure 3. *Elphidium williamsoni* (phylotype S1) isolated from Gullmar fjord (Sweden). **A.** Scanning electron micrograph. **B-F.** TEM micrographs. **B, C and D**. Overviews of different chambers showing intact (c) and degraded (c*) kleptoplasts situated immediately below the host periphery (B and C) or close to it (D). **E and F**. Kleptoplasts with pyrenoid (py), lamella (la) and thylakoids (th). In F, note the fibrillar vacuole (fv), the multivesicular bodies (mvb) and the degraded lipid droplet (li*) near the kleptoplast. **Scale bars:** A = 100 µm, B- D = 5 µm, and E, F = 1µm.

Figure 4. *Elphidium oceanense* (phylotype S3) isolated from Bourgneuf Bay (France). **A.** Scanning electron micrograph. **B.** Light micrograph of semi-thin section. **C-F.** TEM micrographs. **C.** Overview of a chamber showing kleptoplasts (c) and vacuoles (v) evenly and densely distributed in the endoplasm. Also noted are the nucleus (n), pore plates (pp) and organic lining (ol). **D.** Kleptoplasts (c) often in degradation or perforated in large vacuoles (v). **E and F.** Higher magnification views showing

Kleptooplasts, often in degraded state, with pyrenoid (py), lamella (la) and thylakoids (th). **Scale bars:** A, B = 50 µm, C = 10 µm, D = 2 µm, E = 1 µm and F = 0.5 µm.

Figure 5. *Elphidium selseyense* (phylotype S5) isolated from Wadden Sea (Texel, Netherlands). **A.** Scanning electron micrograph. **B-F.** TEM micrographs. **B, C and D**. Overview of different chambers showing vacuoles (v) and kleptoplasts (c) situated immediately below the host periphery (B-D) with some internally (B). **E and F**. Kleptoplasts with a girdle lamella (gl), a pyrenoid (py), thylakoids (th) and osmiophilic globules (og, possibly plastoglobules). In E, note the Golgi apparatus (g) and electron opaque bodies (eo) near the kleptoplast. **Scale bars:** A = 100 µm, B, C = 5 µm, D = 2 µm, and E, F = 1 µm.

Figure 6. *Elphidium* aff. *E. crispum* isolated from Yugawara (Kanagawa Prefecture, Japan). **A.** Scanning electron micrograph. **B-H.** TEM micrographs. **B.** Overviews showing four different chambers. **C and D**. Kleptoplasts (c) evenly and densely distributed in the endoplasm of the cell and organization of surrounding vacuoles (v) and organelles. **D**. Mitochondria (m), digestive vacuole (dv), Golgi apparatus (g), peroxisome (p). **E.** Kleptoplast with a girdle lamella (gl), thylakoids (th), pyrenoid (py) divided in two by a lamella (la) and osmiophilic globules (og, possibly plastoglobules). **F.** Kleptoplasts (c) in the endoplasm. **G and H.** Intact (c) and degraded (c*) kleptoplasts. **Scale bars:** A = 100µm, B = 50 µm, C = 4 µm, D, E, G = 1 µm, F = 5 µm, and H = 2 µm.

Figure 7. *Planoglabratella opercularis* isolated from Yugawara (Kanagawa Prefecture, Japan). **A.** Scanning electron micrographs of dorsal (upper), lateral (middle) and ventral (lower) views. **B.** Transmission electron micrograph montage showing chambers and organization of kleptoplastids at the cell periphery. **Scale bars:** A = 100 µm and B = 25 µm.

Figure 8. Transmission electron micrographs of *P. opercularis.* **A-B**. Organization of the kleptoplasts (c) situated immediately below the host periphery close to the pore plates (pp) as well as in the endoplasm but at a lower density. Note the surrounding organelles: mitochondria (m), Golgi apparatus (g), nucleus (n) and nucleolus (nu), and also the pores (po), pore plates (pp), the organic lining (ol) and osmiophilic globules (og, possibly plastoglobules). **C and D.** Details of peripheral kleptoplasts showing thylakoids (th) and pyrenoids (py) and also the foraminiferal pores (po), pore plates (pp), and the organic lining (ol). **E and F.** Kleptoplasts (E) in the endoplasm with surrounding organelles (F): mitochondria (m), peroxisome (p). **Scale bars:** A, D = 2 µm, B = 5 µm, C, E, F = 1 µm.

Figure 9. *Ammonia sp.* (phylotype T6) from Bourgneuf Bay (France). **A.** Scanning electron micrograph. **B.** Transmission electron micrograph overview of a chamber of *Ammonia aomoriensis* showing kleptoplasts (c), empty diatom frustules (d), vacuoles (v), pores (po), pore plates (pp), organic lining (ol) and former location of the test (t). **C.** Light micrograph of semi-thin section. **D.** Transmission electron micrograph of a diatom in the endoplasm of the foraminifer, showing diatom organelles: kleptoplast (c), nucleus (n), vacuoles (v), mitochondria (m) and frustules (f). **Scale bars:** A, C = 100 µm, B = 50 µm, and D = 5 µm.

Figure 10. Transmission electron micrographs of *Ammonia sp.* (phylotype T6). **A and B.** Organization of kleptoplasts (c) showing pyrenoids (py), lamella (la) and lamella surrounding the pyrenoid (lp), and thylakoids (th). **C and D.** Kleptoplasts in degradation (c*). Note the lipids (li) in the foraminifer. **Scale bars:** A, C, D = 2 µm, B = 1 µm.

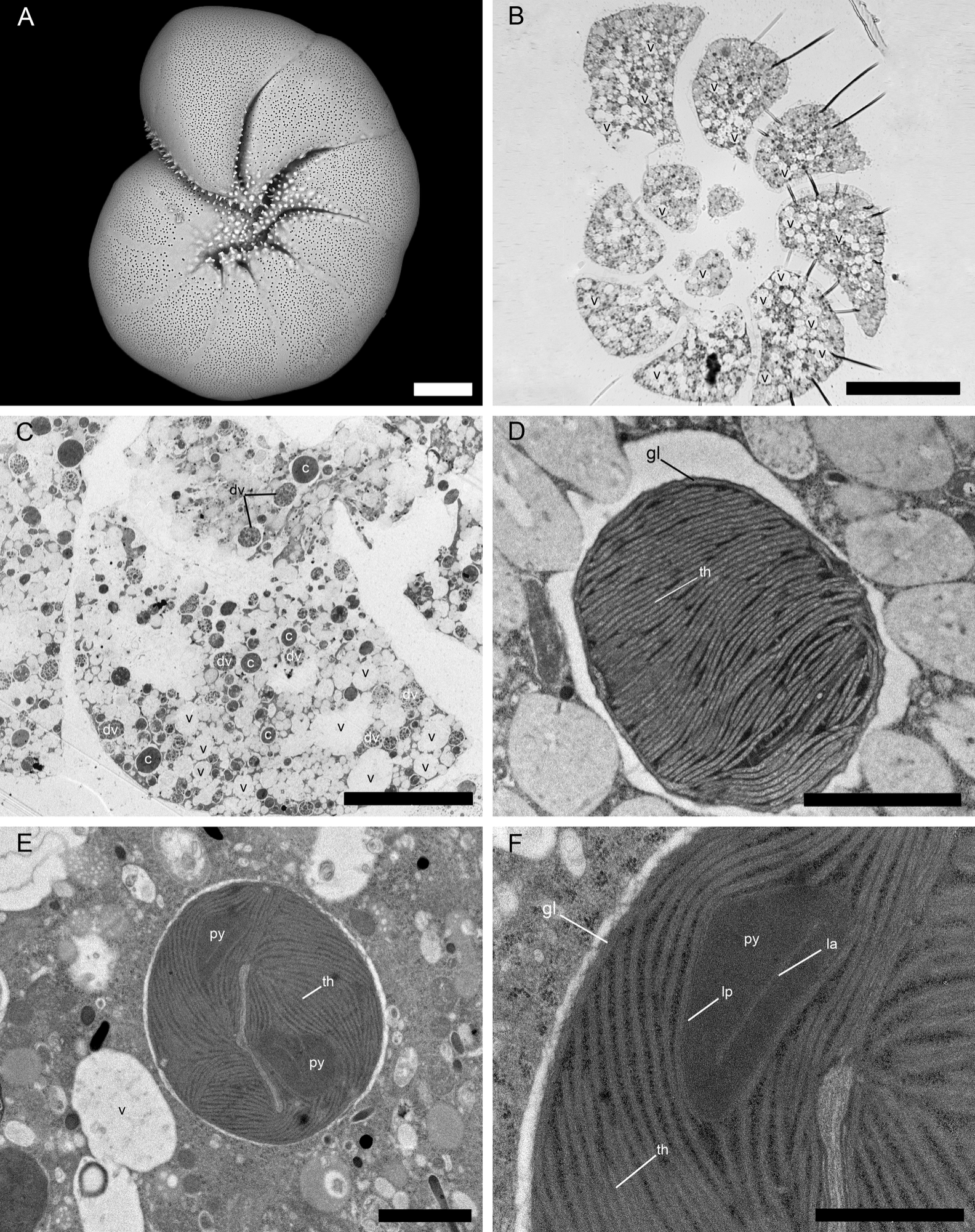
A
B
v
C
c
dv
D
gl
th
E
py
th
py
v
F
gl
py
la
lp
th

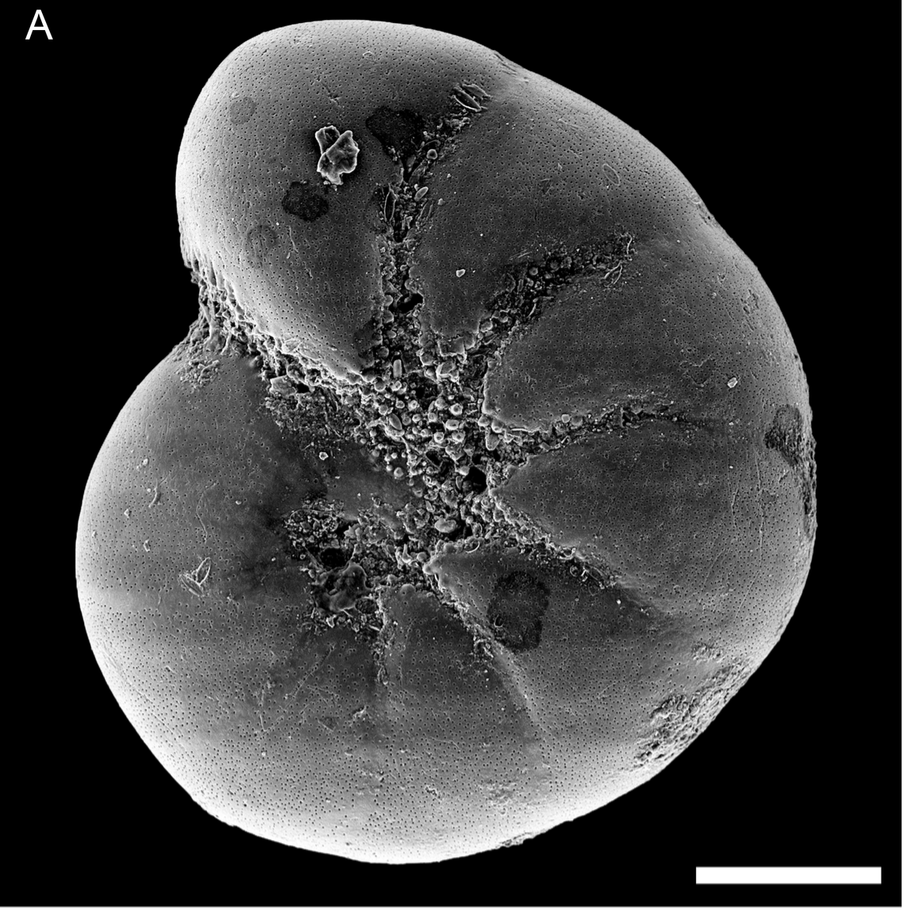
A

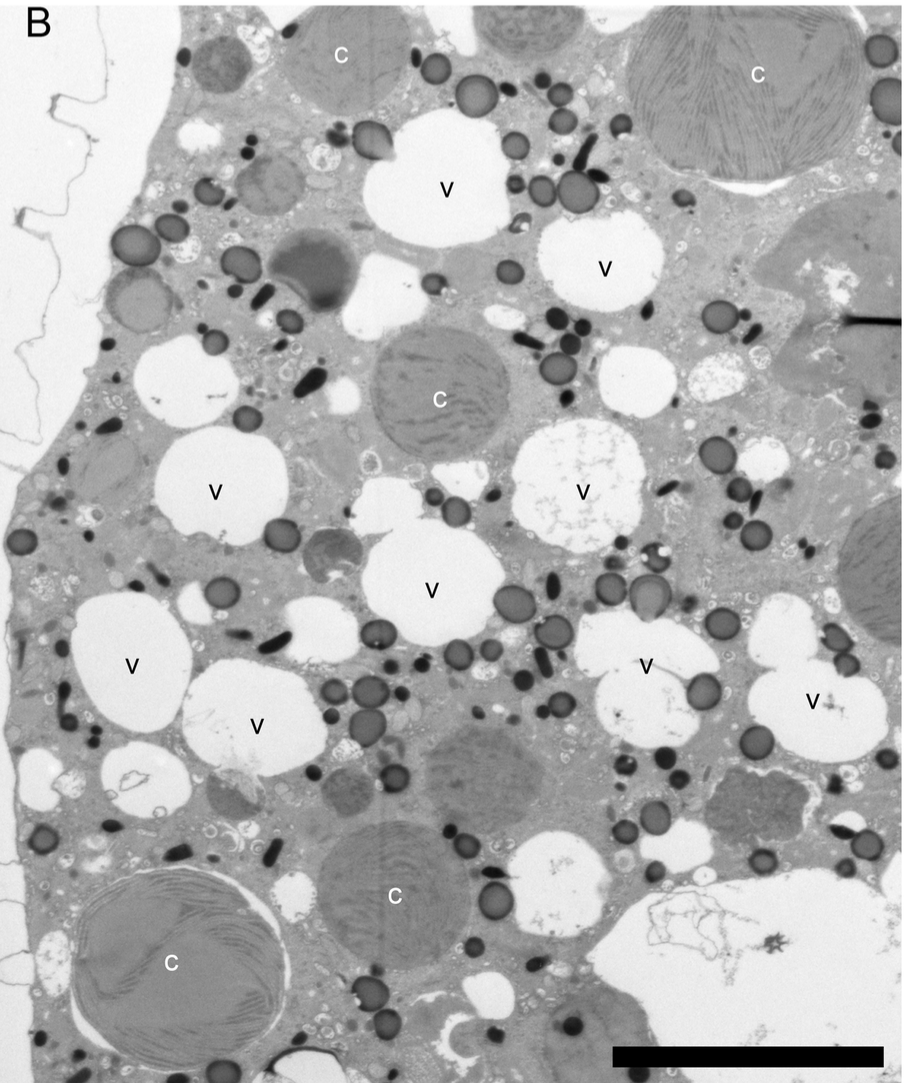
B
c
c
v
v
c
v
v
v
v
v
v
v
c
c

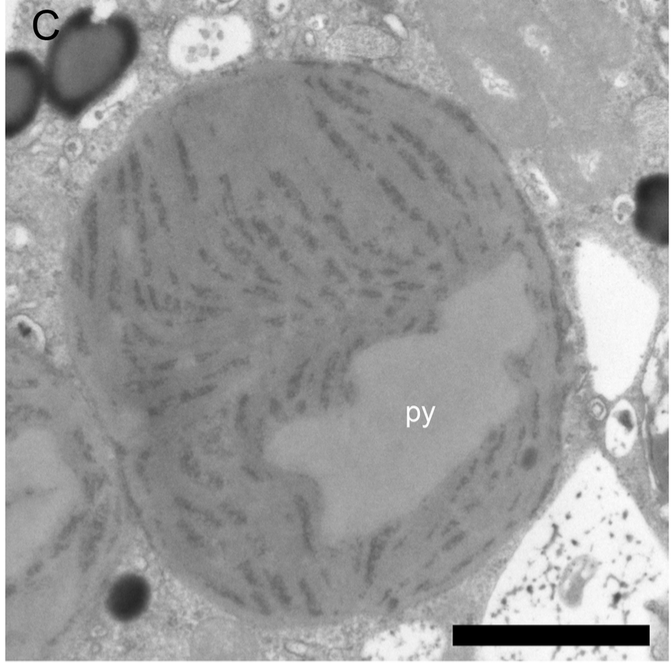
C
py

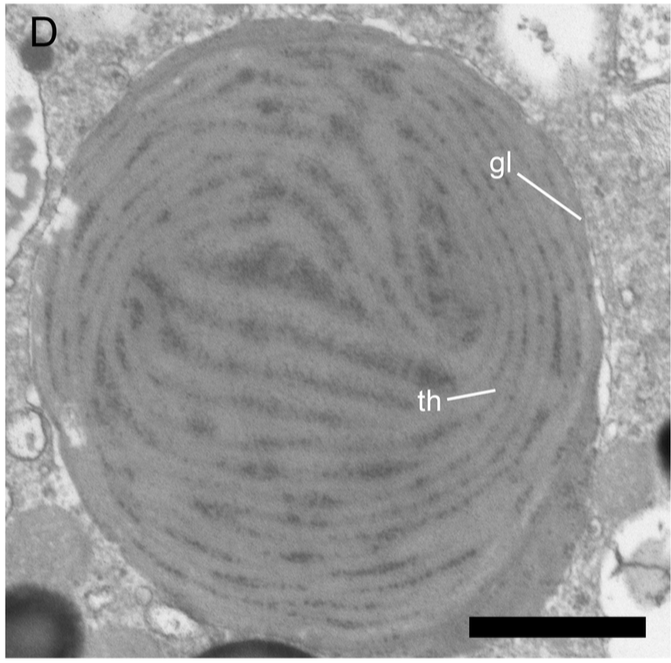
D
gl
th

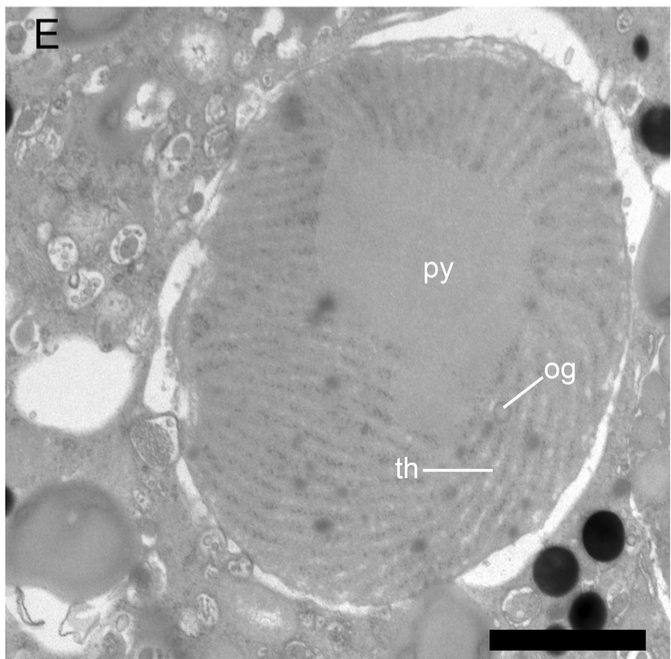
E
py
og
th

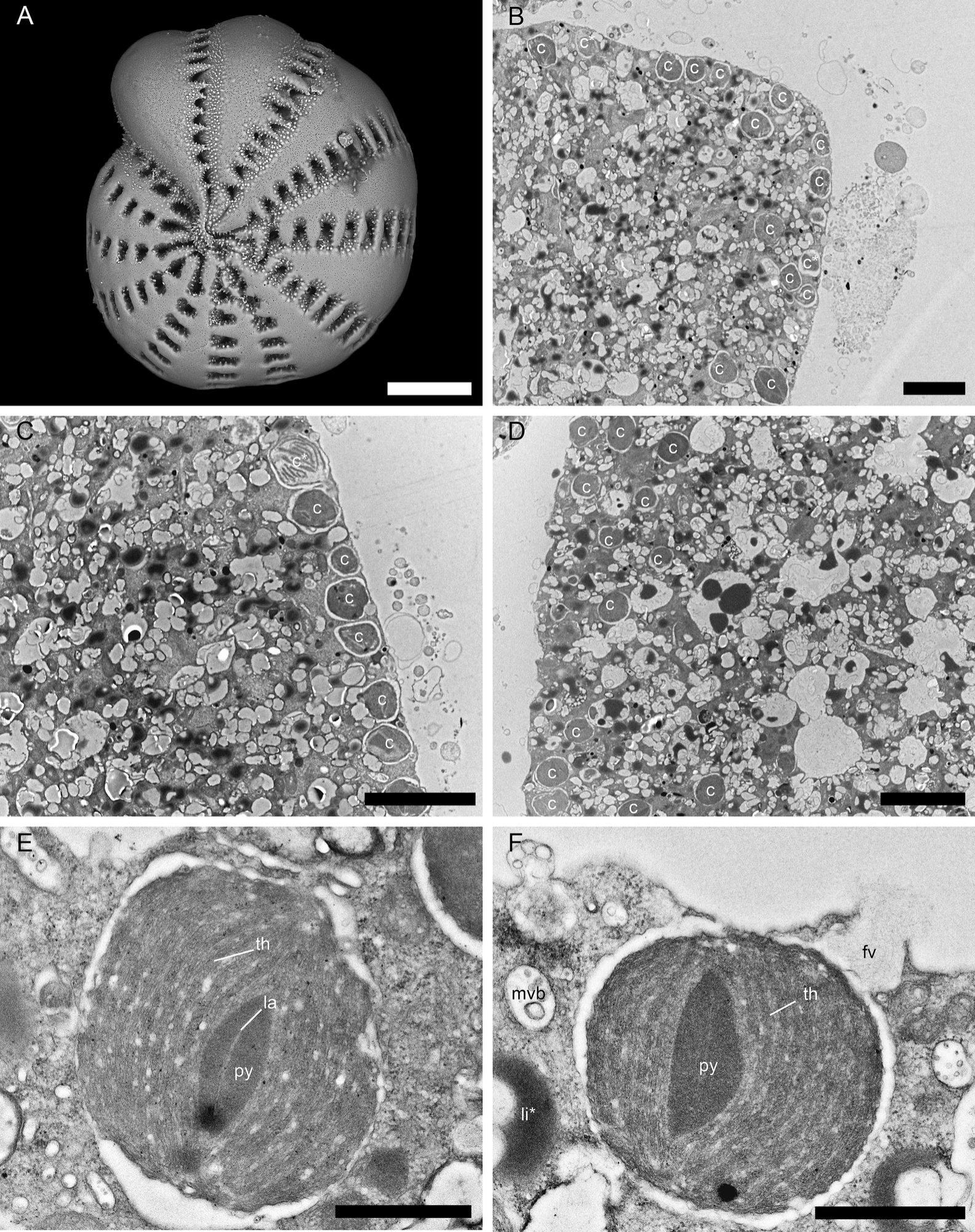
A
B
C
C*
D
E
th
la
py
F
fv
mvb
th
py
li*

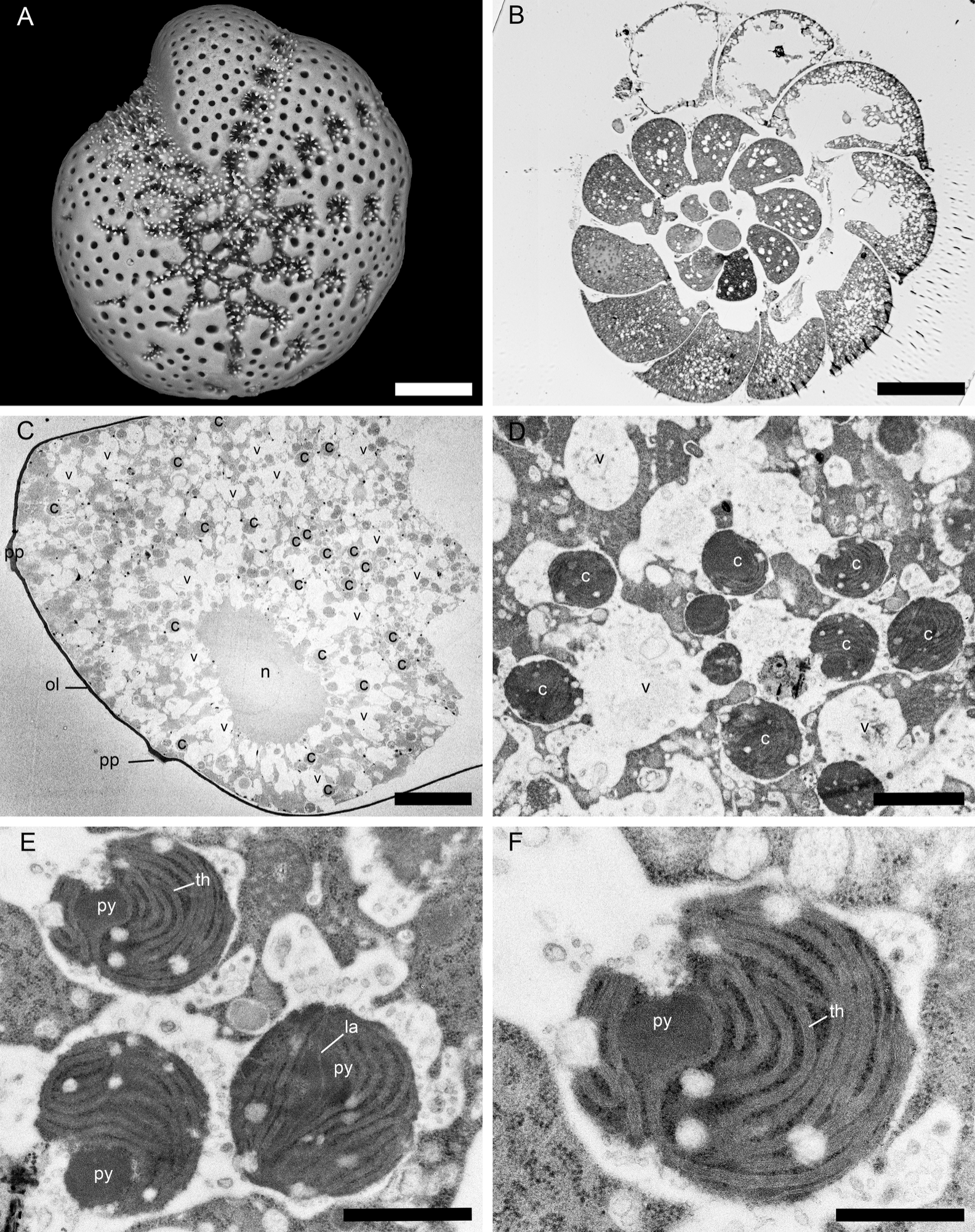
A
B
C
c
v
pp
n
ol
pp
D
c
v
E
th
py
la
py
py
F
py
th

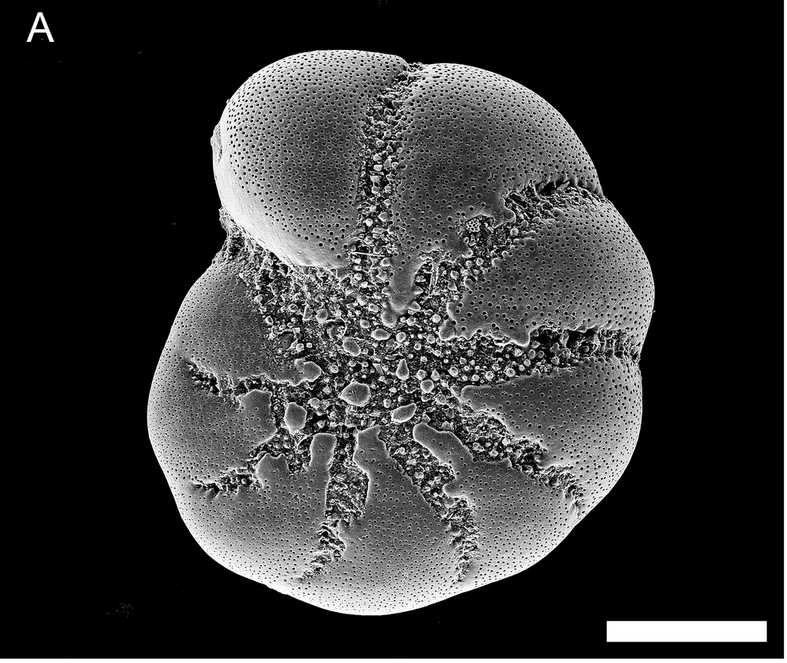
A

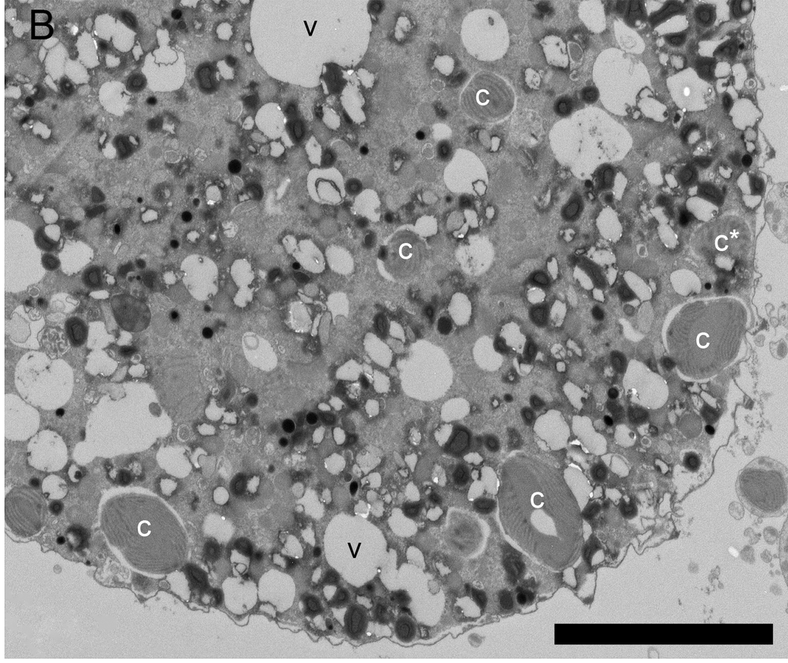
B
v
c
c
c*
c
c
c
v

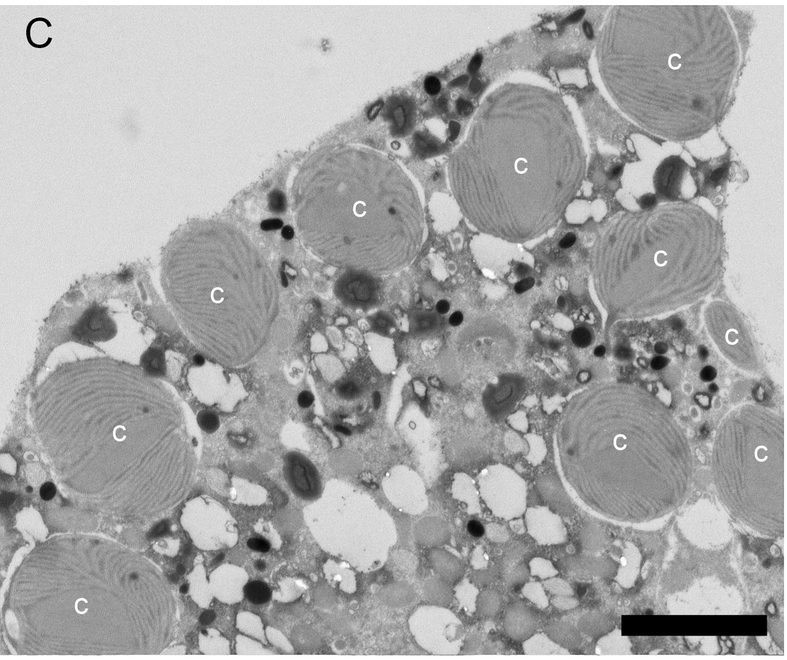
C
c
c
c
c
c
c
c
c
c
c
c

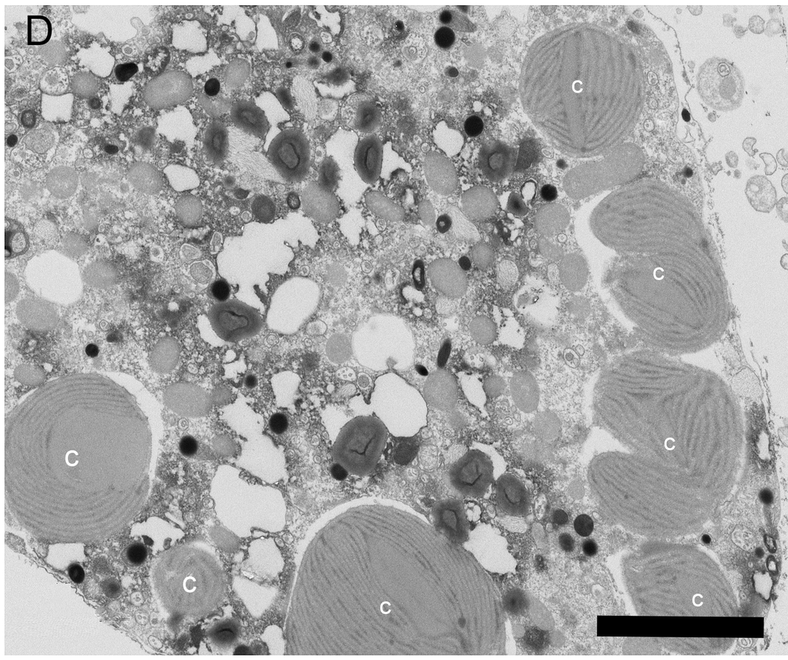
D
c
c
c
c
c
c
c
c

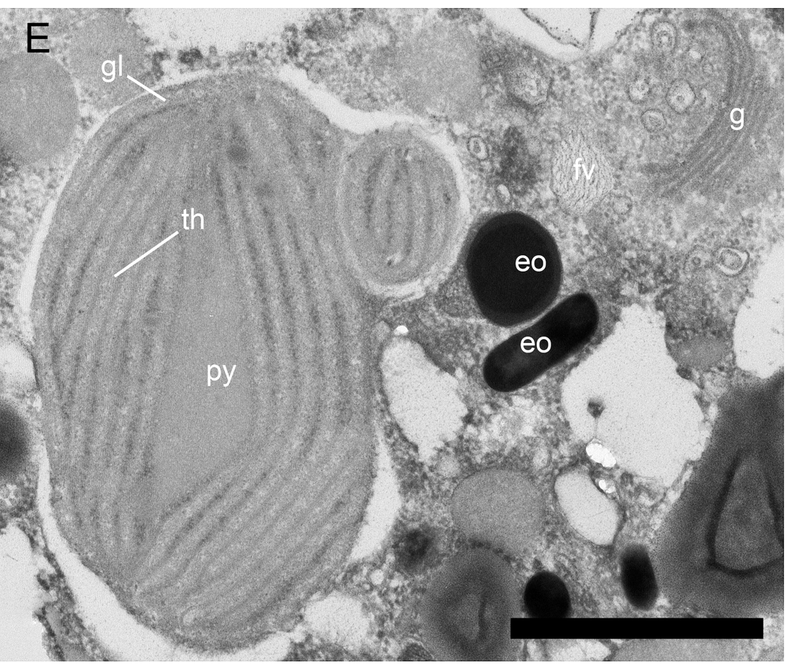
E
gl
g
fv
th
eo
eo
py

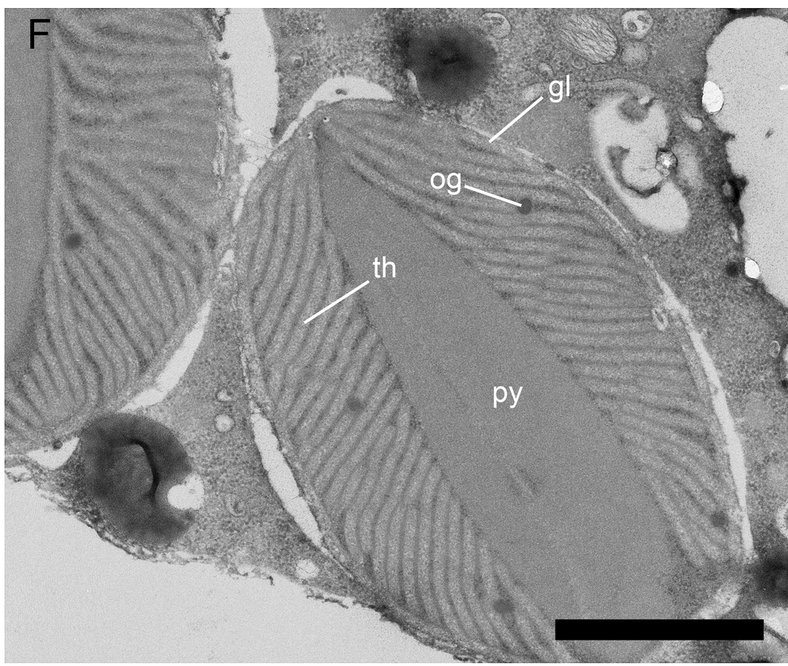
F
gl
og
th
py

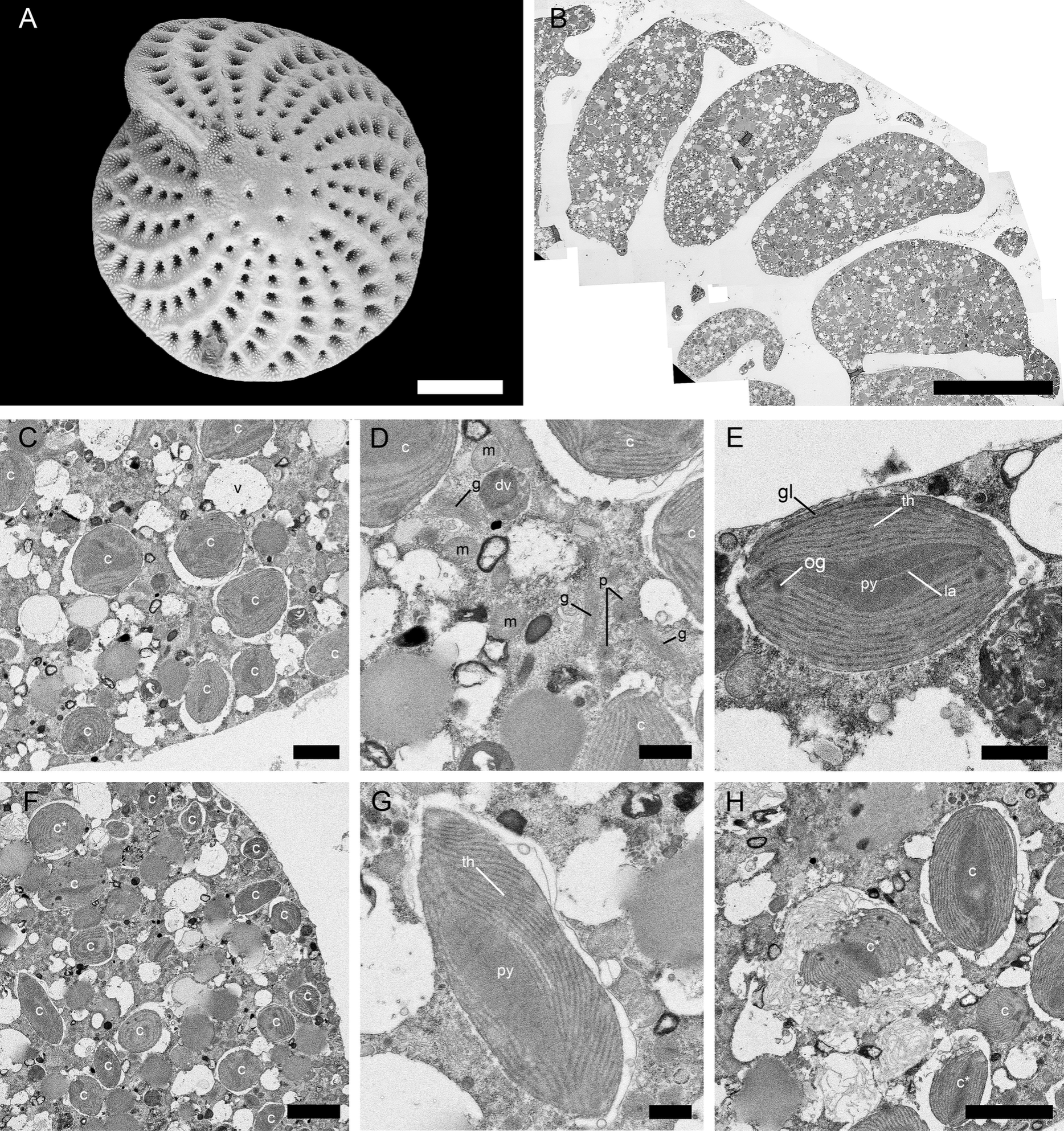
A
B
C
c
v
D
m
g
dv
p
E
gl
th
og
py
la
F
c*
G
H

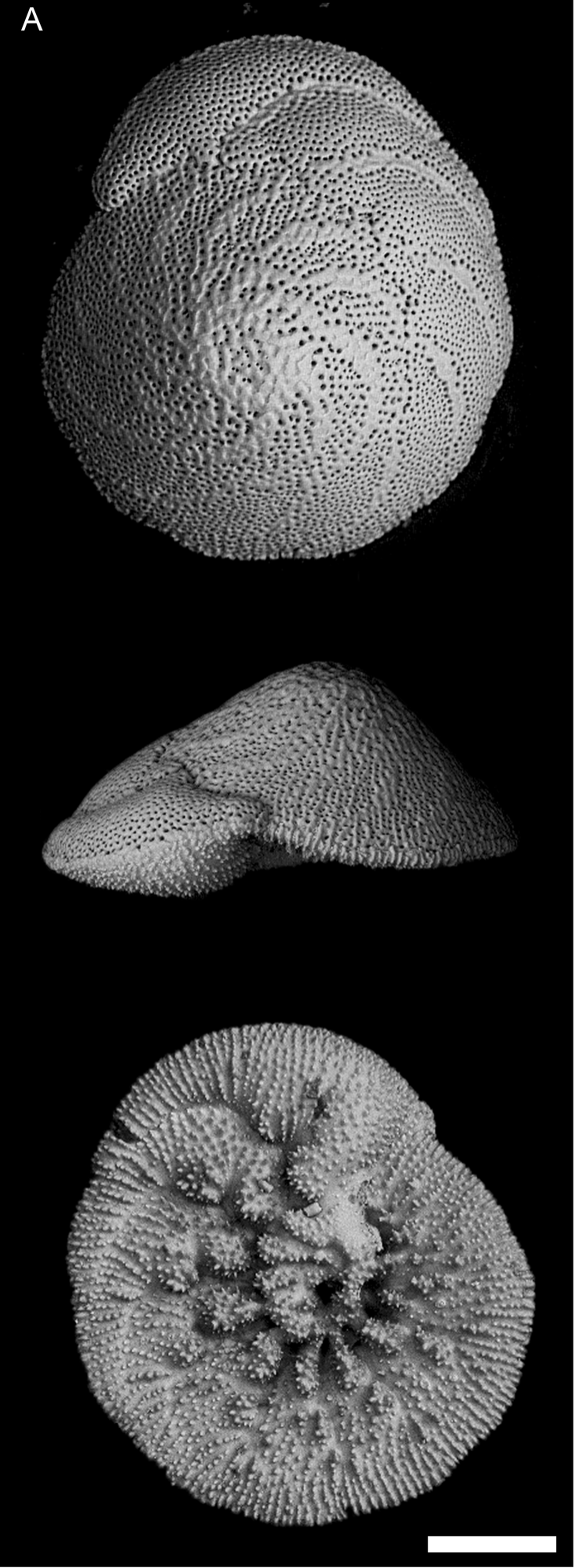
A

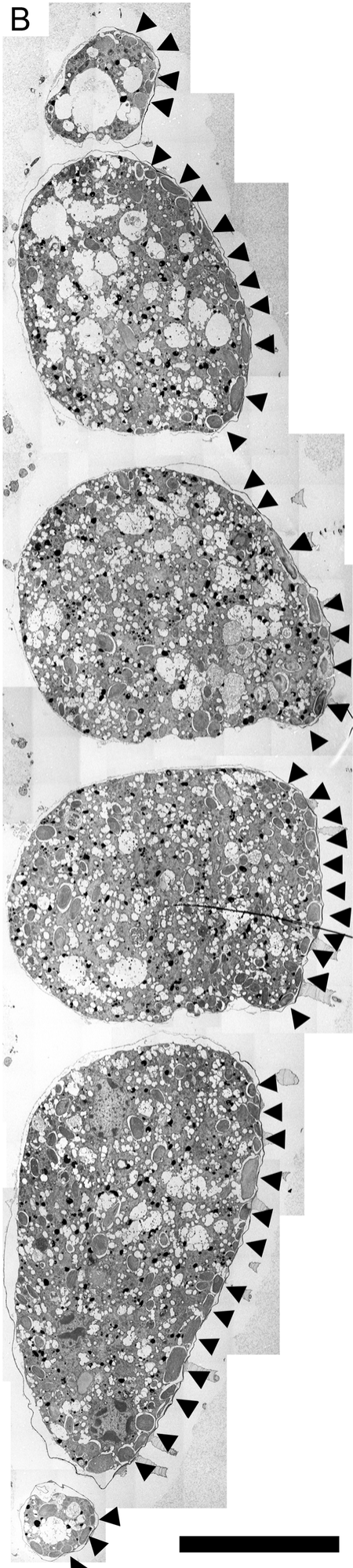
B

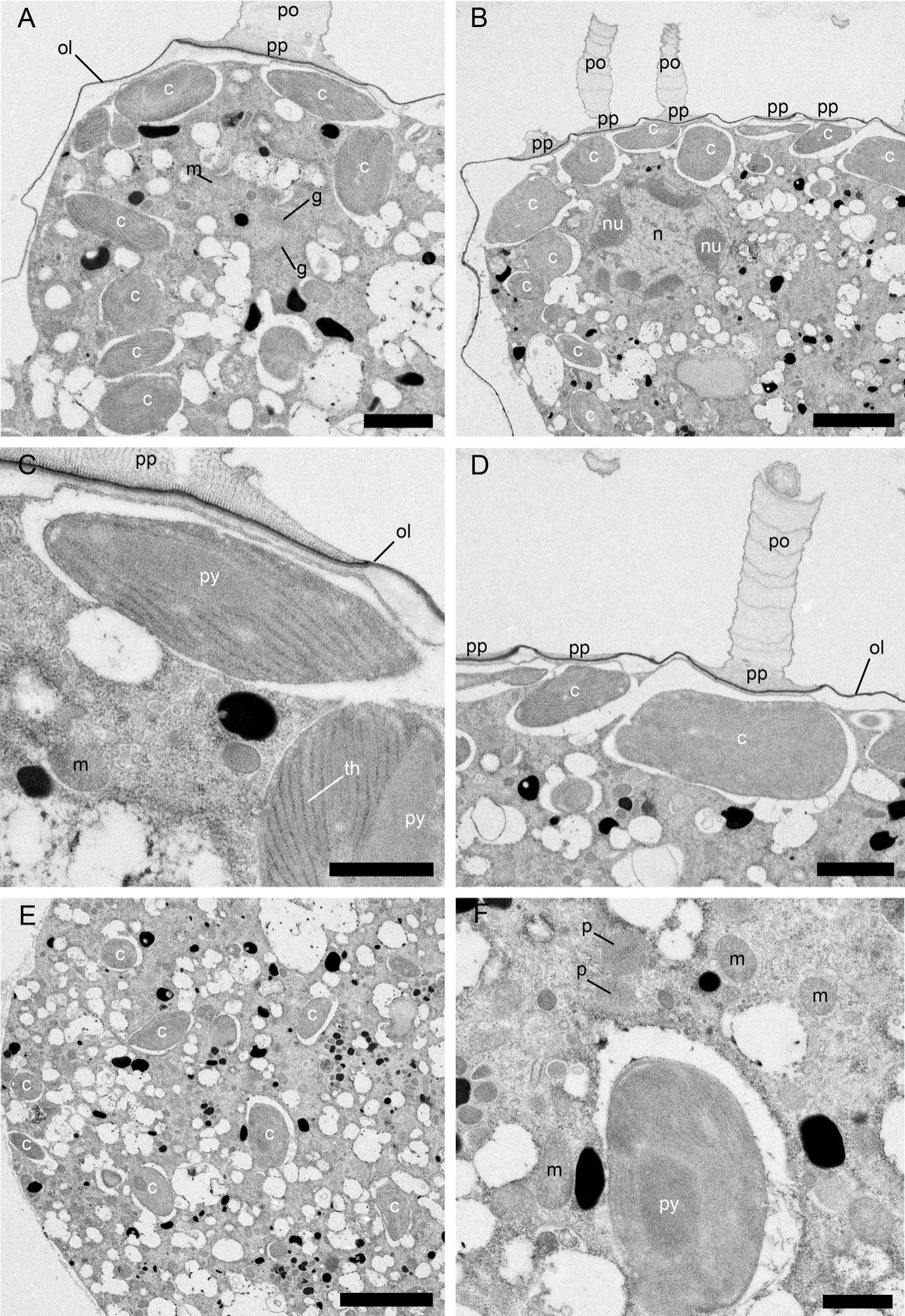
A
po
ol
pp
c
m
g
B
po
pp
nu
n
C
pp
ol
py
m
th
D
po
pp
ol
E
F
p
m
py

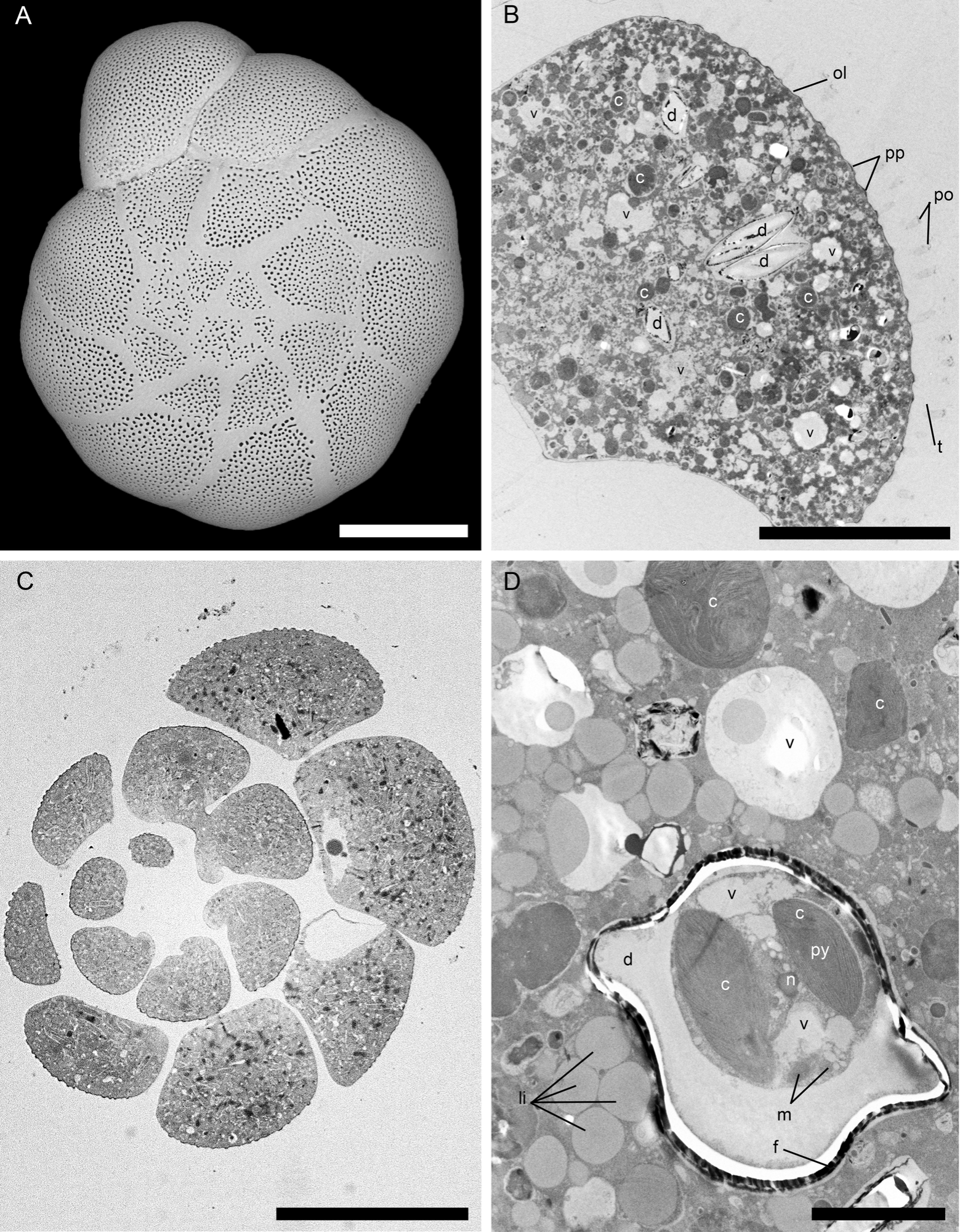
A
B
ol
pp
po
t
v
c
d
C
D
py
n
li
m
f

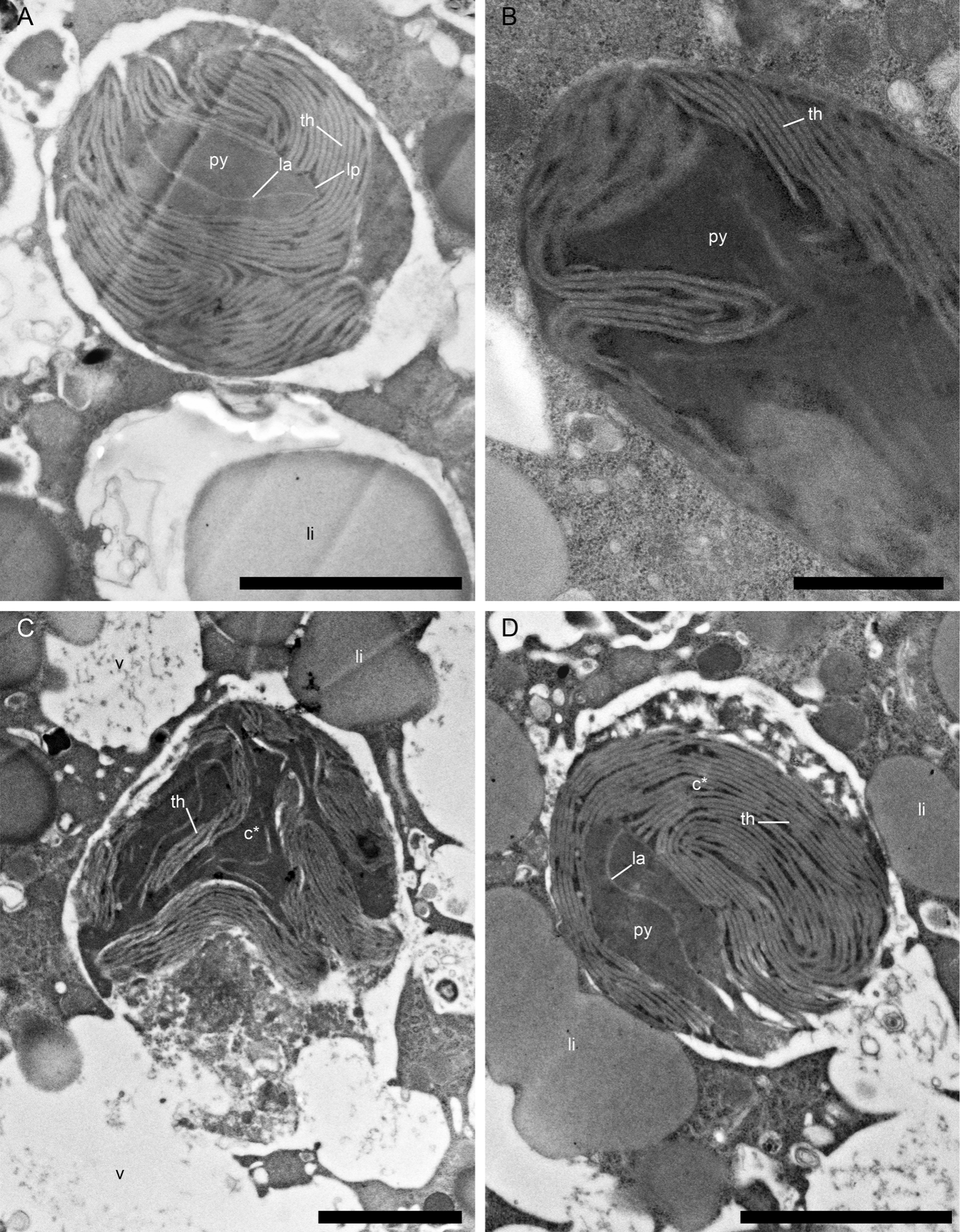
A
th
py
la
lp
li
B
th
py
C
v
li
th
c*
v
D
c*
th
li
la
py
li

Table 1. Available DNA sequences for specimens from the same population or the same location as TEM studied specimens. The phylotype names refer to the systems described by Hayward et al. (2004) for *Ammonia* and Darling et al. (2016) for *Elphidium* and *Haynesina*.

Morphospecies	Gene	Phylotype	DNA isolate	Location	Accession number (GenBank)	Reference
Haynesina germanica	SSU	S16	H17-16	Bourgneuf (FR)	KY347799	present study
Haynesina germanica	SSU	S16	6008	Den Oever (NL)	EF534074	Schweizer et al., 2008
Haynesina germanica	SSU	S16	F323	Den Oever (NL)	GQ853557	Schweizer et al., 2011
Elphidium williamsoni	SSU	S1	GF191	Gullmar Fjord (SE)	KY347798	present study
Elphidium oceanense	SSU	S3	Bn130	Bourgneuf (FR)	KY347797	present study
Elphidium selseyense	SSU	S5	1244	Mokbaai (NL)	GQ853558-59	Schweizer et al., 2011
Planoglabratella opercularis	SSU	N/A	N/A	Omaezaki (JP)	Z69614	Pawlowski et al.. 1997
Planoglabratella opercularis	ITS	A1	GO17	Ooura Cove, Shimoda (JP)	AF498333	Tsuchiya et al. 2003, 2014
Planoglabratella opercularis	LSU	N/A	GO17	Ooura Cove, Shimoda (JP)	AF194044	Tsuchiya et al., 2000
Ammonia aomoriensis	SSU	T6	H17-34	Bourgneuf (FR)	KY347800	present study

Table 2. Synopsis of the ecology, sequestered plastid abundance, plastid distribution and other specifics for seven species of benthic foraminifera from shallow-water photic habitats.

Foraminiferal species	Ecology	Relative plastid abundance*	Plastid length (maximum dimension)	Plastid distribution	Other specifics
Haynesina germanica (S16)	Tolerant to variations in temperature and salinity, often encountered in Lusitanean and Boreal waters, in shallow intertidal to subtidal habitats (Alve and Murray, 1999; Darling et al., 2016)	Abundant	2-5 µm	Evenly distributed in the endoplasm	Presence of both healthy and degraded sequestered plastids Single plastids surrounded by host membrane
Elphidium williamsoni (S1)	Tolerant to variations in temperature and salinity, commonly encountered in shallow intertidal to subtidal habitats of Lusitanian and Boreal waters (Alve and Murray, 1999; Darling et al., 2016)	Abundant	2-3 µm	Mainly distributed at the periphery of the endoplasm and also globally distributed but at lower density	Single plastids surrounded by host membrane
Elphidium oceanense (S3)	Tolerant to large variations in temperature and salinity, only marginally encountered in shallow intertidal to subtidal Lusitanian and Boreal waters in sediment with high organic content (Alve and Murray, 1999; Darling et al., 2016)	Abundant	1-2 µm	Evenly distributed in the endoplasm	Plastids often appeared degraded with small circular electron-lucent disruption of thylakoids and pyrenoids Numerous sequestered plastids per vacuole
Elphidium selseyense (S5)	Widespread and opportunistic species, tolerant to variations of temperature and salinity in shallow intertidal to subtidal Lusitanean and Boreal waters (Darling et al., 2016; Horton and Edwards, 2006; Murray, 1991)	Abundant	2-3 µm	Mainly distributed at the periphery of the endoplasm and globally but at lower density	Single plastids surrounded by host membrane
Elphidium aff. *E. crispum*	Commonly encountered in the intertidal zone of rocky shores around the Japanese Islands, living on coralline algae (Kitazato, 1994)	Abundant	4-8 µm	Evenly distributed in the endoplasm	Single plastids surrounded by host membrane
Planoglabratella opercularis	Commonly encountered in the intertidal zone of rocky shores around the Japanese Islands where it lives on thalli of coralline algae (Tsuchiya et al., 2014). It has an attached and mobile form, and graze on epiphytic diatoms (Kitazato 1988)	Abundant	3-5 µm	Situated immediately below the dorsal foraminiferal periphery, close to pores and pores plates, forming a continuous layer of chloroplasts and also globally in the endoplasm but at lower density	One to three plastids surrounded by host membrane
Ammonia aomoriensis (T6)	Typical intertidal species in Europe and East Asia, tolerant to variations of temperature and salinity, found in tidal flats, marshes and brackish lakes (Hayward et al., 2004)	Rare	2-3 µm	Evenly distributed in the endoplasm	Diatom frustules with or without their cellular content Occurrence of both healthy and degraded plastids

* The results of this column are based on visual observations and literature data (Lopez et al., 1979; Correira and Lee, 2002; Goldstein et al., 2004; Cesbron et al. 2017)